Low Temperature Plasma Technology

Methods and Applications

Edited by
Paul K. Chu
XinPei Lu

CRC Press
Taylor & Francis Group

Low Temperature Plasma Technology

Low Temperature Plasma Technology

Methods and Applications

Edited by
Paul K. Chu
XinPei Lu


CRC Press
Taylor & Francis Group
Boca Raton London New York

CRC Press is an imprint of the
Taylor & Francis Group, an **informa** business

CRC Press
Taylor & Francis Group
6000 Broken Sound Parkway NW, Suite 300
Boca Raton, FL 33487-2742

Version Date: 20130214

International Standard Book Number-13: 978-1-4665-0991-7 (eBook - PDF)

Contents

SECTION III Applications

Preface

During the last few decades, low-temperature plasmas, especially atmospheric pressure plasmas, which are driven by several urgent applications including plasma medicine and treatment of biocompatible materials, have attracted much attention. In order to meet the ever-increasing requirements, novel methods have been proposed since the mid-1990s, for example, using nanosecond voltage pulses rather than DC or kHz AC voltages to drive the plasmas, generating plasmas by using confined microdischarge gaps, and generating plasma in open space (plasma jets). At the same time, in order to better understand the various plasma characteristics, there have been major advances in plasma diagnostics such as cavity ringdown spectroscopy and laser-induced fluorescence methods. On the heels of these developments, applications of low-temperature plasmas have been extended to various fields, including nanomaterials, environment, liquid treatment, biocompatible materials treatment, and plasma medicine.

The objective of this book is to summarize recent technological advances and research in the rapidly growing field of low-temperature plasmas and their applications. The book is intended to provide a comprehensive overview of the related phenomena such as plasma bullets, plasma penetration into biofilms, the discharge mode transition of atmospheric pressure plasmas, self-organization of microdischarges, and so on. It also describes relevant technology and diagnostics such as nanosecond pulsed discharge, cavity ringdown spectroscopy, laser-induced fluorescence measurement, and also fast-developing research on atmospheric pressure nonequilibrium plasma jets. Finally, applications of low-temperature plasmas, including synthesis of nanomaterials, environmental applications, treatment of biomaterials, and plasma medicine will be discussed. All in all, this book will provide a balanced and thorough treatment of the core principles, relevant novel technologies and diagnostics, and state-of-the-art applications of low-temperature plasmas.

Although the book focuses mainly on low-temperature plasmas and related topics, the scope of this book is actually quite wide. In order to ensure high quality, we are very happy to have renowned authors from many different countries including Italy, the Netherlands, Belgium, the United States, France, Slovakia, Singapore, and the People's Republic of China. These authors are pioneers in the respective fields. For example, Prof. Schoenbach, the contributor of Chapter 5 on high-pressure microcavity discharges, was the first to report stable high-pressure operation of microdischarges, even in air, in a cylindrical hollow cathode geometry. His group innovated the term "microhollow cathode discharges (MHCDs)" for these discharges, and it is well adopted by others to describe the three-layer configuration. Other contributors such as Profs. Y.N. Wang, D.Z. Wang, C.O. Laux, S. De Benedictis, C. Wang, C. Leys, S.Y. Xu, B.R. Locke, K.P. Yan, and X.Y. Liu have been known for decades for their excellent contributions to their fields.

This book is intended for graduate students and scientists working in low-pressure plasmas, atmospheric pressure plasmas, plasma diagnostics, plasma nanotechnology, and plasma medicine.

It is written at a level appropriate for graduate education in low-temperature plasma physics and materials science and has relevance in biology, chemistry, and engineering. The book also constitutes an excellent advanced reference for senior college students who want to pursue research in these topics on the graduate level.

XinPei Lu and Paul K. Chu
Editors

Editors Note

Paul K. Chu received his BS in mathematics from the Ohio State University in 1977 and his MS and PhD in chemistry from Cornell University in 1979 and 1982, respectively. He is Chair Professor of Materials Engineering in the Department of Physics and Materials Science in City University of Hong Kong. Paul's research activities are quite diverse, encompassing plasma surface engineering and various types of materials and nanotechnology. Professor Chu has coedited 8 books on plasma science, biomedical engineering, and nanotechnology, special issues in *IEEE Transactions of Plasma Science* and *Surface and Coatings Technology*, as well as MRS proceedings. He has coauthored more than 30 book chapters, 1100 journal papers, and 800 conference papers. He has also been granted numerous patents in the United States, Europe, and the People's Republic of China. He is chairman of the Plasma-Based Ion Implantation and Deposition (PBII&D) International Committee and member of the Ion Implantation Technology (IIT) International Committee and IEEE Nuclear and Plasma Science Society Fellow Evaluation Committee. He is fellow of the IEEE, APS, AVS, MRS, and HKIE (Hong Kong Institution of Engineers), senior editor of *IEEE Transactions on Plasma Science*, and associate editor of *Materials Science & Engineering Reports*. Professor Chu is also an editorial board member of international journals that include *Biomaterials, Plasma Sources Science and Technology*, and *Surface and Coatings Technology*, and he has won a number of awards, including the 2007 IEEE NPSS Merit Award.

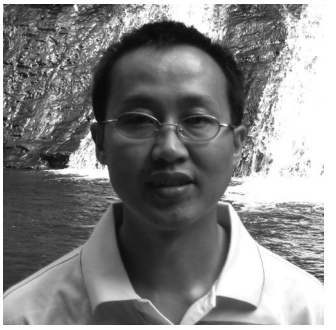

XinPei Lu received his PhD in electrical engineering from the Huazhong University of Science and Technology, Hubei, People's Republic of China. Upon graduation, he worked at Old Dominion University as a research associate for 4 years. In 2007, he joined Huazhong University of Science and Technology, where he is now a professor (Chang Jiang Scholar) with the College of Electrical and Electronic Engineering. He is a senior member of IEEE. He has also served as a guest editor for *IEEE Transactions on Plasma Science* and as a session chair at the International Conference on Plasma Science since 2007. He has given many invited talks at international conferences, including the IEEE International Conference on Plasma Science. His research interests include low-temperature plasma sources and their biomedical applications, modeling of low-temperature plasmas, and plasma diagnostics. He is the author or coauthor of about 50 peer-reviewed journal articles and holds six patents in these areas.

Contributors

Peter J. Bruggeman
Department of Applied Physics
Eindhoven University of Technology
Eindhoven, the Netherlands

Huiliang Cao
Shanghai Institute of Ceramics
Chinese Academy of Sciences
Shanghai, People's Republic of China

Santolo De Benedictis
CNR Istituto di Metodologie Inorganiche e dei Plasmi
Unità Organizzativa di Supporto di Bari
Bari, Italy

Nathalie De Geyter
Department of Applied Physics
Ghent University
Ghent, Belgium

Giorgio Dilecce
CNR Istituto di Metodologie Inorganiche e dei Plasmi
Unità Organizzativa di Supporto di Bari
Bari, Italy

Peter Dubruel
Department of Organic Chemistry
Ghent University
Ghent, Belgium

Mario Janda
Department of Astronomy, Earth Physics and Meteorology
Comenius University
Bratislava, Slovakia

Chunqi Jiang
Department of Electrical Engineering
University of Southern California
Los Angeles, California

Wei Jiang
School of Physics
Huazhong University of Science and Technology
Hubei, People's Republic of China

Christophe O. Laux
Department of Astronomy, Earth Physics and Meteorology
Comenius University
Bratislava, Slovakia

Christophe Leys
Department of Applied Physics
Ghent University
Ghent, Belgium

DaWe Liu
State Key Laboratory of Advanced Electromagnetic Engineering and Technology
Huazhong University of Science and Technology
Hubei, People's Republic of China

Xuanyong Liu
Shanghai Institute of Ceramics
Chinese Academy of Sciences
Shanghai, People's Republic of China

Bruce R. Locke
Department of Chemical and Biomedical Engineering
Florida State University
Tallahassee, Florida

XinPei Lu
State Key Laboratory of Advanced Electromagnetic Engineering and Technology
Huazhong University of Science and Technology
Hubei, People's Republic of China

Zdenko Machala
Department of Astronomy, Earth Physics and Meteorology
Comenius University
Bratislava, Slovakia

Rino Morent
Department of Applied Physics
and
Department of Organic Chemistry
Ghent University
Ghent, Belgium

David Z. Pai
Department of Astronomy, Earth Physics and Meteorology
Comenius University
Bratislava, Slovakia

Karl H. Schoenbach
Frank Reidy Research Center for Bioelectrics
Old Dominion University
Norfolk, Virginia

Jizhong Sun
Department of Physics
Dalian University of Technology
Dalian, People's Republic of China

Chuji Wang
Department of Physics and Astronomy
Mississippi State University
Mississippi State, Mississippi

Dezhen Wang
Department of Physics
Dalian University of Technology
Dalian, People's Republic of China

Yanhui Wang
Department of Physics
Dalian University of Technology
Dalian, People's Republic of China

You-nian Wang
School of Physics and Optoelectronic Technology
Dalian University of Technology
Dalian, People's Republic of China

Shaoqing Xiao
NIE and Institute of Advanced Studies
Nanyang Technological University
Singapore

Shuyan Xu
NIE and Institute of Advanced Studies
Nanyang Technological University
Singapore

Keping Yan
Department of Chemical and Biological Engineering
Zhejiang University
Hangzhou, People's Republic of China

Yu-ru Zhang
School of Physics and Optoelectronic Technology
Dalian University of Technology
Dalian, People's Republic of China

Haiping Zhou
NIE and Institute of Advanced Studies
Nanyang Technological University
Singapore

I

Fundamentals

1

Introduction

DaWe Liu
and XinPei Lu

1.1 A Historical Perspective of Plasma

Plasmas make up more than 99% of visible matter in the universe. They consist of positive ions, electrons or negative ions, and neutral particles. Plasma is regarded as the fourth state of matter. When a solid (the first state of matter) is heated, the particles in it get sufficient energy to loosen their structure and thus melt to form a liquid (the second state of matter). After obtaining sufficient energy, the particles in a liquid escape from it and vaporize to gas (the third state of matter). Subsequently, when a significant amount of energy is applied to the gas through mechanisms such as an electric discharge, the electrons that escape from atoms or molecules not only allow ions to move more freely but also produce more electrons and ions via collisions after accelerating rapidly in an electric field. Eventually, the higher number of electrons and ions change the electrical property of the gas, which thus becomes ionized gas or plasma (Figure 1.1).

The study of plasmas can be traced to the seventeenth century. Natural plasmas such as lightning and polar lights are often observed and have intrigued people for many centuries. The desire to understand the mechanism governing plasma generation led to the invention of the discharge device by early researchers.

Although the fact that frictional charge induces discharges was first observed by Greek philosophers, the mechanism of plasma production was not understood until the seventeenth and eighteenth centuries. Figure 1.2a shows an early discharge device made by Anders; the apparatus consists of a glass sphere that can be rapidly spun on an axle by a great wheel.[1] The axle is hollow and connected to a globe through a valve on the other end to a vacuum pump. A glow appeared when the sphere was spun in the dark. Later on, the phenomena of static electricity and discharge became a subject for study. In 1734 Priestley described a "pencil of electric light," today known as corona discharge.[2] Around the same time, significant progress in the development of electric charge storage devices such as Leyden batteries made it possible to study spark discharges. Figure 1.2b shows a spark discharge device[3] that consists of two metal electrodes and a charge storage device known as the Leyden jar. The short-circuit connection between the two metal electrodes caused the quick discharge of the stored charge, resulting in sparks. Later in 1800, an electrochemical battery was invented by Volta.[4] Petrov discovered continuous arc discharge in 1803 using a sufficiently powerful electric battery.[5]

During the nineteenth century, significant progress was made with regard to electric energy storage and vacuum systems. Faraday developed the direct current (DC) glow discharge, the forerunner to today's vacuum plasma, by applying voltage up to 1000 V to an evacuated tube (~1 Torr) in 1831–1835.[6]

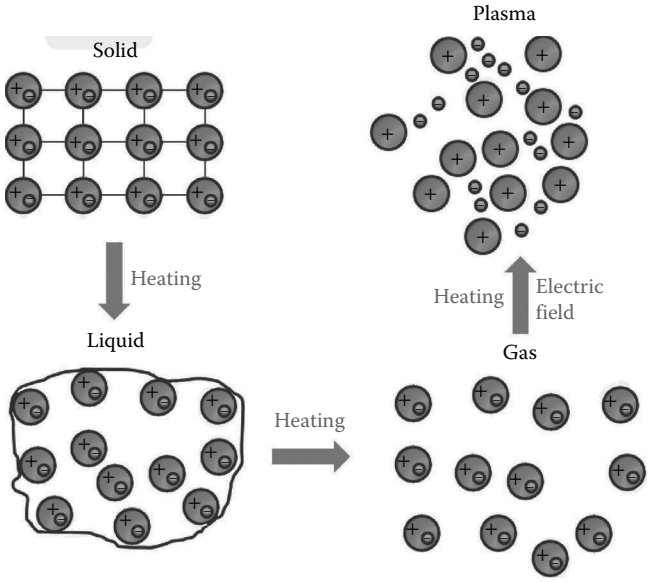

FIGURE 1.1 The transition of states of matter on application of heat.

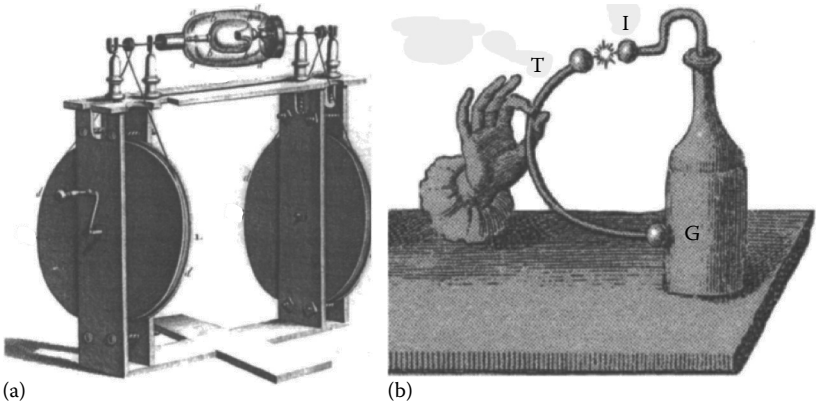

FIGURE 1.2 (a) A glow discharge device developed in 1705. (From Anders A., *IEEE Trans. Plasma Sc.,* 31, 1052, 2003.) (b) An arc discharge device developed in 1775. (From Dibner, B., *Galvani-Volta: A Controversy That Led to the Discovery of Useful Electricity,* Burndy Library, 1952.)

Plasma was first identified as radiant matter by Sir William Crookes in 1879.[7] In the second half of the nineteenth century and the early twentieth century, significant understanding about gas discharges was achieved. J. Townsend studied gas discharge in a uniform electric field and came up with the Townsend discharge theory.[8] He laid the foundation of modern plasma research. His contribution also included the discoveries of cross sections of various electron–atom collisions, drift velocities of electrons and ions, and their recombination coefficients. Later in 1920s, Langmuir not only came up with the term "plasma,"[9] but also invented the Langmuir probe to determine the electron temperature, electron density, and electric potential of a plasma.[10]

The twentieth century witnessed rapid progress in the development, diagnostics, and applications of plasma. Low-pressure radio-frequency (RF) plasma produced in a vacuum chamber is being used intensively in basic processing such as for deposition and etching in the semiconductor industry since the 1970s. Since the 1990s the application of atmospheric pressure plasma eliminated the need for expensive

vacuum chamber and pumping systems; as such, atmospheric pressure plasmas are being widely used for environmental applications, surface modification of materials, biomedical applications, and so on.

1.2 Types of Plasma

Plasma is composed of electrons, positive ions, and neutral particles, and can be described based on the ionization degree, density, thermodynamic equilibrium, and so on; therefore, plasma is classified in many different ways.

1.2.1 Plasma Ionization

The ionization degree is defined as $\alpha_i = N_i/(N_i + N_n)$, where N_i is the number density of ions and N_n is the number density of neutrals. The response of any plasma to a magnetic field and the electric conductivity of plasma are determined by α_i. Plasma with $10^{-6} < \alpha_i < 10^{-1}$ is weakly ionized. Because the degree of ionization is determined by the electron temperature in the plasma, weakly ionized plasma is also referred to as low-temperature plasma. In most plasma-processing chambers, the degree of ionization is less than 10^{-4}. The degree of ionization of inductively coupled plasma (ICP) and electron cyclotron resonance is a lot higher, about 10^{-2}. Plasma with $\alpha_i \approx 1$ is fully ionized, and is referred to as "hot" plasma. Examples include fusion plasmas, solar wind (interplanetary medium), and stellar interiors (the Sun's core).

1.2.2 Plasma Densities

1.2.2.1 High-Density Plasma (High-Pressure Plasma)

High-density plasma refers to plasma with particle density $N > 10^{15-18}$ cm^{-3}. The high number of ions and free radicals of high-density plasma not only enhance excitation/ionization collisions but also increase the ion bombardment rate. Therefore, high-density plasmas generated by ICP and capacitively coupled plasma (CCP) are often used for etching in microelectronics, producing nanomaterials, decontaminating plasmas, and so on.

1.2.2.2 Low-Density Plasma (Low-Pressure Plasma)

Low-density plasma refers to plasma with particle density $N < 10^{12-14}$ cm^{-3}. Unlike in the case of high-density plasma, the collision rate between particles of low-density plasma is negligible. Low-density plasma is used in the laser wakefield accelerator,[11] where plasma density must be low enough to allow propagation of lasers of optical or infrared frequencies.

1.2.3 Plasma Thermal Equilibrium

On the basis of relative temperature between electrons, ions, and neutrals, plasmas are classified as *thermal equilibrium*, *local thermal equilibrium*, or *nonthermal equilibrium*.

1.2.3.1 Thermal Equilibrium Plasma

The electron temperature (T_e), ion temperature (T_i), and neutral temperature (T_n) are identical in thermal equilibrium plasma. This is attributed to the frequent collisions between electrons and ions/neutrals inside high-temperature and high-density plasma. Examples include the natural fusion reactor (Sun), a magnetic field (of tokamak design), or inertial (laser) confinement of a plasma.

1.2.3.2 Nonthermal Equilibrium Plasma

In nonthermal equilibrium plasma, the momentum transfer between light electrons and heavy particles (ions and neutrals) is not efficient and the power applied to plasma favors electrons; therefore, the electron

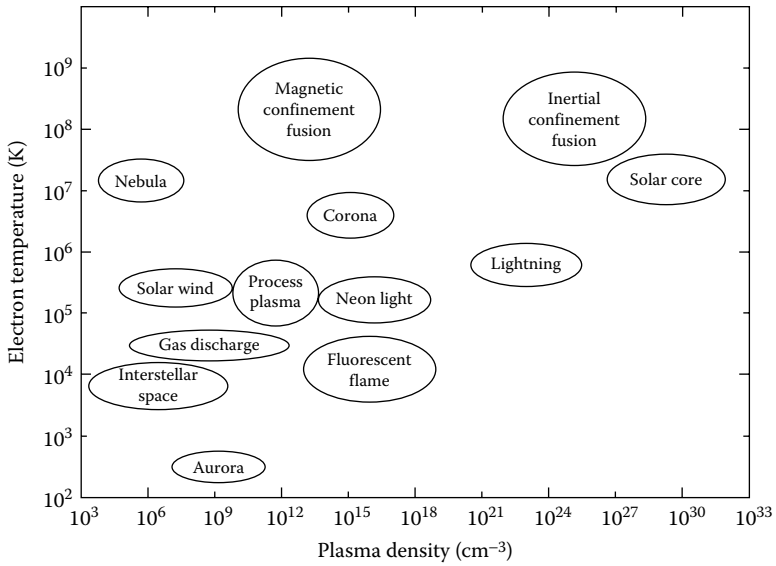

FIGURE 1.3 Typical parameters of naturally occurring and laboratory plasmas.

temperature (T_e) is considerably higher than in ions (T_i) and neutrals (T_n), that is, $T_e >> T_i, T_n$. Nonthermal equilibrium plasmas are generated by corona discharge, glow discharge, arc discharge, capacitively coupled discharge, inductively coupled discharge, wave heated plasma, and so on. Applications of nonthermal plasma have expanded to cover a large number of fields including environmental engineering, aeronautics and aerospace engineering, biomedicine, textile technology, and analytical chemistry.

1.2.3.3 Local Thermal Equilibrium Plasma

Unlike thermal equilibrium plasma and nonthermal equilibrium plasma, local thermal equilibrium plasma is in quasi-equilibrium: the electron, positive ion, and neutral temperatures are in the same range. The ion temperature of local thermal equilibrium plasma is 3,000–10,000 K (0.4–1 eV), which is much higher than that of nonthermal plasma, but its electron temperature is much lower (0.4–1 eV compared with 2–10 eV of nonthermal plasma). Local thermal equilibrium plasma can be generated by DC and RF arcs, or by an inductively coupled torch. They are used for plasma spraying (coating) and thermal plasma chemical and physical vapor deposition.

Figure 1.3 shows the typical parameters for naturally occurring and laboratory plasmas. Gas discharge and process plasmas have been discussed in this book. Their densities are in the range of 10^7–10^{14} cm^{-3}, and their electron energy is in the range of 1–100 eV.

1.3 Plasma Diagnostics

The oldest and frequently used diagnostic tool for low-temperature plasmas is the Langmuir probe. Since the 1920s, when the probe was invented by Irving Langmuir and his coworkers to measure DC plasma properties,[10] it has been developed for measurement under more general conditions such as for pulsed DC,[12] RF,[13] and microwave plasmas.[14] The Langmuir measurement is based on I–V characteristics of the Debye sheath, that is, the current density flowing to the surface of a plasma as a function of the voltage drop across the sheath. Detailed analysis of the I–V characteristics can yield primary plasma parameters: plasma density, plasma potential, floating potential, electron temperature, and electron energy distribution function (EEDF). More details on special arrangements and practical considerations of the Langmuir probe can be found in Chung et al.,[15] Huddlestone and Leonard,[16] Hutchinson,[17] and Lieberman and Lichtenberg.[18]

Active spectroscopy such as cavity ring-down spectroscopy (CRDS) and laser-induced fluorescence (LIF) provide highly sensitive ways to measure absolute density of plasma species. CRDS involves a laser that is used to illuminate a high-finesse optical cavity, which consists of a simple setup of two highly reflective mirrors. After the intensity of the laser builds up in the cavity due to constructive interference, the laser is turned off, so light is reflected between the two mirrors thousands of times and decays exponentially. After the plasma is introduced inside the cavity, the plasma species absorbs light, so the intensity of light decreases faster. The "ring-down time" is obtained by measuring the time needed by the light to decrease to 1/e of its initial intensity, and is used to calculate the density of plasma species.[19] After decades of development, plasma-CRDS (P-CRDS) has evolved into a powerful plasma diagnostic tool. Different laser sources, namely, continuous and pulsed wave lasers, are used to analyze various plasmas such as an ICP and a microwave-induced plasma; the absolute number density of many plasma species in time and in space are determined thus.[20–23] More details on configurations of an experimental P-CRDS and coupling of P-CRDS with OES for plasma diagnostics can be found in Chapter 8.

The LIF technique provides an efficient way to measure the ground state and long-lived, nonradiative, excited atoms, molecules, or radicals.[24] This technique has been used for many years for diagnostics in plasmas. It includes two major steps. The first one is to excite the atoms or molecules in the ground state (E_1) to a higher energy level (E_3) through resonant absorption of laser photons, with $E_3 - E_1 = h\upsilon_{laser}$. Afterward, the excited state comes down to a lower energy state E_2, by emitting fluorescence, with $E_2 - E_1 = h\upsilon_{LIF}$. The LIF system consists of a laser source, an arrangement of lenses, a fluorescent medium (plasma), collection optics, and a detector.[25] The popular laser sources for LIF are the Nd:YAG laser, dye lasers, excimer lasers, and ion lasers. The laser light passes through a set of lenses and mirrors to illuminate the plasma. Subsequently, the signal is captured by the charged coupled device (CCD) camera. A timing trigger device is usually used to synchronize the laser source and detectors. Two-photon absorption LIF (TALIF), as the name suggests, is the absorption of two photons followed by fluorescence of the third photon.[26,27] Due to the second-order effect, two-photon absorption is much weaker than single-photon absorption, but forbidden transition probabilities and vacuum ultraviolet (VUV) laser requirements make TALIF an alternative to single-photon absorption to investigate the ground-state species.[28–31] A quantitative description of the role of the collision process in plasma, calibration of LIF, and LIF measurement of active species in thermal plasma can be found in Chapter 9.

1.4 Applications of Plasma

The most common man-made plasmas in our daily life are plasma lamps. The fluorescent lamp and high-intensity arc lamp are primarily two types of plasma light sources.[32] The fluorescent lamp is a gas discharge lamp that uses electricity to excite mercury vapor. The UV light produced by mercury atoms causes a phosphor to fluoresce and produces visible light. The energy conversion efficiency of fluorescent lamps is a lot higher than that of incandescent lamps, so they are used as an energy-saving alternative in homes.[33] The high-intensity arc lamp produces light by means of an electric arc between tungsten electrodes housed inside a transparent quartz tube. Its color characteristics depend on the gaseous elements in the tube. They are widely used in commercial settings, especially for advertisement lighting in public areas. The plasma display panel is a technique based on fluorescent lamps. A panel typically has millions of tiny cells in the compartmentalized space between two panels of glass. The UV photons produced by the plasma strike on the phosphor that is painted on the inside of the cell. Different colors can be obtained depending on the type of phosphor used. Three cells comprising the primary colors of visible light constitute each pixel in the display panel. Varying the signal voltage to the cells thus results in different color outputs.[34] Compared with light-emitting diode (LED) display and liquid crystal display (LCD), plasma display has better color fidelity and wider viewing angles. A quantitative description on plasma light sources can be found in Chapter 5.

Plasma application is also an effective, cheap, and environmentally friendly process for the disinfection and degradation of organic pollutants in water. Compared with the traditional chlorination process, the ozonation process has stronger oxidization efficiency and no side effects. Siemens' ozonizer based on air

corona discharge has been successfully used for ozone synthesis in many industrial fields for more than 150 years without any major modification.[35,36] Instead of *ex situ* discharge for ozone synthesis, the *in situ* discharge inside water or in close proximity to a water surface can produce more chemically active species such as H_2O_2, $O^{\bullet}$, $OH^{\bullet}$, HO_2^*, O_3^*, N_2^*, e^-, O_2^-, O^-, and O_2^+.[36] Most of these species have even stronger oxidation potential than that of ozone. Therefore, dielectric barrier discharge (DBD), contact glow discharge electrolysis, and silent discharges are used for water treatment through direct electrical discharge. Furthermore, the strong electric field and UV radiation caused by these discharges are also lethal to several kinds of microorganisms present in water.[37] More details on plasma water purification and discharges in liquids can be found in Chapters 11 and 12.

The removal of NO_x from a mobile device is of growing concern in nonthermal plasma processing for air pollution control. Unlike removal of NO_x from a stationary source, this involves chemical reduction of NO_x to N_2 molecule rather than oxidation to HNO_2 or HNO_3. The plasma-driven catalysis reactor with a TiO_2 catalyst greatly enhances NO_x removal efficiency to 95% under proper plasma power.[35] Moreover, large-scale facilities for nonthermal plasma processing have been set up in Poland, China, Korea, and Japan. For the waste gas with flow rate of 35,000 $Nm^3\ h^{-1}$, 70% removal rate of NO_x and 99% removal rate of SO_2 were achieved through plasma driven by 160 kW pulse power. DC + AC driving plasmas are also being considered for large-scale applications.[35] A quantitative description of environmental applications can be found in Chapter 11.

Due to the high bactericidal effectiveness and ease of access into narrow and confined spaces, plasma has been used for decades for packaging in the food industry, sterilization of surgery equipment, and blood coagulation. Recently, the development of low-temperature (<40°C) atmospheric pressure plasma sources extended plasma treatment applications.[38] Low-temperature plasma can combat fungal diseases efficiently and propagate through socks; therefore, 25–40% of the population with tinea pedis infection can be treated effectively with appropriate plasma devices.[39] Contact-free plasma is also an ideal candidate for normal dental care, because it can clean out bacteria in the teeth cavity without drilling, which reduces the patient's suffering a lot.[40] Moreover, for chronic wounds caused by venous diseases, arterial diseases, diabetes mellitus, and carcinoma, although plasma cannot cure the underlying disease, by eliminating bacterial and fungal infection, it can support the treatment and speed up recovery. Finally, the development of hand plasma sterilization devices provides a fast and efficient way to sterilize public buildings including hospitals, children nurseries, nursing homes, and so on.[38] More details on plasma medicine can be found in Chapter 14.

1.5 Organization of This Book

There are three major sections of this book. After the introductory chapter, Chapter 2 proceeds to provide the reader with necessary theoretical foundations in nonthermal plasmas at atmospheric pressure. The next section, "Processing and Characterization" consisting of seven chapters (Chapters 3–9), educates readers about an advanced plasma laboratory. Phenomena such as plasma bullets, plasma penetration into biofilms, discharge mode transition of atmospheric pressure plasmas, self-organization of microdischarges are introduced. The numerical diagnostics by particle-in-cell/Monte Carlo (PIC/MC) and fluid/hybrid models and experimental diagnostics through CRDS and the LIF measurement are presented. The final section, "Applications of Plasmas," consisting of six chapters (Chapters 10–15), not only discusses important practical applications such as environmental protection, treatment of biomaterials, and plasma medicine, but also summarizes research challenges and future trends associated with these applications. The book is a suitable degree-level text for students of engineering and science, and a research monograph for practicing engineers and scientists. In the remainder of this section, each chapter is examined one by one.

Chapter 3 presents general properties of atmospheric pressure thermal plasmas, as well as methods for their generation are discussed. Then, a complete description of atmospheric pressure nonthermal

plasmas, including their general properties, instabilities of diffuse discharges and stabilization mechanisms, and different types of discharges, is presented.

Chapters 3 and 4 illustrate how the theoretical formulations on plasma physics and plasma chemistry presented in Chapter 2 are incorporated into the computational model. For the modeling of low-pressure plasmas, the principles, capabilities, and limitations of fluid/hybrid and PIC/MC models are reviewed and compared. For the modeling of atmospheric pressure plasmas, besides a detailed discussion on theoretical models and computation details, the studies on discharge mode transition and nonlinear behaviors through the modeling are also presented.

Chapter 5 begins with a review of electrode geometries and materials and fabrication techniques. The modes of operation, electrical characteristics, and microplasma parameters including gas temperature, electron density, and electron energy are highlighted. The chapter then turns to parallel operation, series operation, and OES diagnostics of microplasmas. The large surface-to-volume ratio of microplasmas not only results in higher energy coupling efficiency with the surroundings than the other discharge methods but also promotes a series of applications, including light sources, plasma reactors, plasma cathodes, thrusters, detectors, and biomedicals, which are described in the final section.

Chapter 6 reviews a pulsed power strategy for plasma generation. The mechanism of pulsed discharge plasmas and their advantages over conventional DC and AC discharge plasmas are highlighted. Different kinds of pulsed discharge sources such as pulsed corona, DBD, spark, and discharges in water are discussed. A detailed description of nanosecond repetitively pulsed (NRP) discharges, including NRP discharge regimes and their transition from corona and glow to spark, gas heating mechanism of NRP, and its applications on plasma-assisted combustion, is presented. A limitation of NRP is the necessity of expensive high-voltage pulse generators with high repetitive rates. The chapter then turns to more economic self-pulsed DC-driven discharges with discussions on streamer mechanism, transient spark–repetitive streamer-to-spark transition, self-pulsed discharge with water, and its applications on flue gas cleaning and decontamination.

Chapter 7 begins with a review of the application driving the development of plasma jet during the last two decades. Then, the key parameters such as driven source, electrode structures, and gas temperatures governing the reactivity of a plasma plume are highlighted. A dominant theme in this chapter is the change in the working gas from noble gas to air, in order to promote applications of plasma jet. The modifications in plasma jet structure based on working gas change are also presented. Then, the measurements of reactive species, such as O, OH, NO, and O_3, are discussed, followed by a section detailing plasma plume propagation characteristics.

Chapter 8 presents the experimental configuration details of P-CRDS and prospective applications of P-CRDS. First, the concept CRDS is covered, which is followed by a discussion on the principles of P-CRDS. Configurations of an experimental P-CRDS system, including laser sources, coupling of a plasma with CRDS, and electronics and data acquisition, are discussed. Descriptions of P-CRDS measurements including absolute number density measurements of plasma species and coupling of P-CRDS with OES for plasma diagnostics are presented. The final section in this chapter summarizes P-CRDS applications such as in plasma medicine, plasma-assisted combustion, and materials processing.

Chapter 9 starts with an overview of fluorescence excitation spectroscopy and LIF diagnostics in plasmas at various pressures. Background mathematical expressions of one-photon LIF, two-photon LIF, and optical–optical double-resonance LIF (OODR-LIF) are all presented. The measurements of internal state distributions and absolute density, including data set of quenching, VET and RET design LIF scheme, calibration of LIF for radical detection, calibration by sources of known radical density, calibration by noble gases, and Rayleigh scattering, are discussed. In the end, the applications of LIF measurement are presented, with emphasis on detection of $N_2(A)$ in pulsed DBD and nanosecond discharges by OODR-LIF and one-photon LIF, detection of N and O in DBD and atmospheric pressure plasma jet by TALIF, and drawbacks of LIF measurements.

Chapter 10 reviews the development of plasma nanotechnology in the past decades, highlights the basic principles of plasma nanotechnology, and discusses the condition and the methods required to obtain high-performance nanomaterials by plasma.

Chapter 11 examines gaseous discharges for pollution emission control, including electrostatic precipitation, ozone generation, and streamer corona discharges. Due to the advantage of air plasma generation, corona discharge modes and chemical reactivity are discussed taking into consideration initial radical generation, fine particle charging, and global chemical kinetics and multiple processing. A thorough discussion on power source and streamer corona plasma reactor, including energization methods and circuit technology, matching between power source and reactors, and system development and technical elements, is presented. The state of the art in flue gas cleaning and volatile organic compounds (VOCs) and odor emission abatement are then explained, with emphasis on NO_x, SO_2, and Hg oxidation and removal, plasma-initiated catalysis intensification, and integrated system and industrial demonstration of flue gas cleaning and plasma catalyst hybrid system. The chapter concludes with three sections detailing indoor air cleaning, fuel gas cleaning, and water cleaning, respectively.

Chapter 12 illustrates different types of discharges, including direct discharges in water, discharges in bubbles, discharges with water electrodes, and discharges with added water vapor or aerosol sprays. The physical properties and elementary water-based chemistry of the discharges in liquids are also discussed. Moreover, their applications are reviewed with emphasis on water and gas treatment, high-voltage switching, biomedical applications, and material synthesis and nanoparticle production.

Chapter 13 starts with a general introduction of surface engineering, including the reason for surface modification, surface modification strategies, and different methods to change polymers. A dominant theme discussed in this chapter is the ability of nonthermal plasmas to modify the polymeric surface. A complete description on the principles of plasma surface interactions and recent achievements on plasma surface modifications are presented, which is followed by techniques employed in polymeric surface modification including plasma postirradiation grafting, plasma syn-irradiation grafting, and plasma polymerization. The chapter concludes with a section on trends and future prospects of these techniques.

Chapter 14 presents the historical progression and development of applications of atmospheric pressure plasma on medicine. The plasma-mediated mechanisms for each application, including instrument sterilization, food decontamination, dental disinfection treatment, wound treatment, and dermatological therapy, are discussed. The research challenges and opportunities associated with these applications are also summarized in the end.

Chapter 15 discusses the surface modifications in implantable biomaterials via plasma-based processes. While several materials (316L stainless steel, cobalt–chromium alloys, and titanium-based alloys) are currently in use, titanium alloys are fast emerging as the first choice for the majority of applications. Hence, this chapter focuses on plasma processing of titanium-based materials, which are an ideal choice for orthopedic applications. The chapter is divided into five sections, starting with the requirements to be met in orthopedic implants, surface modification of titanium-based materials by liquid discharging processes, surface modification of titanium-based materials via plasma spraying processes, surface modification of titanium-based materials using plasma-ion implantation processes, and future prospects.

References

1. A. Anders, *IEEE Transactions on Plasma Science* 31, 1052 (2003).
2. J. Priestley, *The History and Present State of Electricity: With Original Experiments* (Dodsley, Johnson and Davenport, Cadell, 1767).
3. B. Dibner, *Galvani-Volta: A Controversy That Led to the Discovery of Useful Electricity* (Burndy Library, 1952).
4. A. Volta, *Philosophical Transactions of the Royal Society of London* 90, 403 (1800).
5. A. Anders, *IEEE Transactions on Plasma Science* 31, 1060 (2003).
6. M. Faraday, Abstracts of the papers printed in the *Philosophical Transactions of the Royal Society of London* 4, 54 (1837).
7. A.V. Engel, *Ionized Gases* (Oxford University Press, London, 1965).
8. Y.P. Raizer, *Gas Discharge Physics*, corrected edition (Springer, Germany, 1991).

9. I. Langmuir, *PNAS* 14, 627 (1928).
10. H.M. Mott-Smith and I. Langmuir, *Physical Review* 28, 727 (1926).
11. E. Liang, *Physics of Plasmas* 13, 064506 (2006).
12. C. Corbella, M. Rubio-Roy, E. Bertran, and J.L. Andújar, *Journal of Applied Physics* 106, 033302 (2009).
13. J. Hopwood, C.R. Guarnieri, S.J. Whitehair, and J.J. Cuomo, *Journal of Vacuum Science Technology A: Vacuum, Surfaces, and Films* 11, 152 (1993).
14. F. Werner, D. Korzec, and J. Engemann, *Plasma Sources Science and Technology* 3, 473 (1994).
15. P.M.-H. Chung, L. Talbot, and K.J. Touryan, *Electric Probes in Stationary and Flowing Plasmas: Theory and Application* (Springer-Verlag, New York, 1975).
16. R.H. Huddlestone and S.L. Leonard, *Plasma Diagnostic Techniques* (Academic Press, New York, 1965).
17. I.H. Hutchinson, *Principles of Plasma Diagnostics* (Cambridge University Press, New York, 2005).
18. M.A. Lieberman and A.J. Lichtenberg, *Principles of Plasma Discharges and Materials Processing* (John Wiley and Sons, Hoboken, 2005).
19. M.J. Thorpe, K.D. Moll, R.J. Jones, B. Safdi, and J. Ye, *Science* 311, 1595 (2006).
20. W.M.M. Kessels, J.P.M. Hoefnagels, M.G.H. Boogaarts, D.C. Schram, and M.C.M. van de Sanden, *Journal of Applied Physics* 89, 2065 (2001).
21. G. Berden, R. Peeters, and G. Meijer, *International Reviews in Physical Chemistry* 19, 565 (2000).
22. R. Engeln, K.G. Letourneur, M.G. Boogaarts, M.C. van de Sanden, and D. Schram, *Chemical Physics Letters* 310, 405 (1999).
23. Y. Duan, C. Wang, and C.B. Winstead, *Analytical Chemistry* 75, 2105 (2003).
24. J. Amorim, G. Baravian, and J. Jolly, *Journal of Physics D: Applied Physics* 33, R51 (2000).
25. G.P. Davis and R.A. Gottscho, *Journal of Applied Physics* 54, 3080 (1983).
26. E. Caussé, P. Malatray, R. Calaf, P. Charpiot, M. Candito, C. Bayle, P. Valdiguié, R. Salvayre, and F. Couderc, *Electrophoresis* 21, 2074 (2000).
27. J.P. Booth, G. Hancock, N.D. Perry, and M.J. Toogood, *Journal of Applied Physics* 66, 5251 (1989).
28. R.E. Walkup, K.L. Saenger, and G.S. Selwyn, *The Journal of Chemical Physics* 84, 2668 (1986).
29. K. Niemi, V.S. der Gathen, and H.F. Döbele, *Plasma Sources Science and Technology* 14, 375 (2005).
30. D.J. Bamford, L.E. Jusinski, and W.K. Bischel, *Physical Review A* 34, 185 (1986).
31. G.D. Stancu, F. Kaddouri, D.A. Lacoste, and C.O. Laux, *Journal of Physics D: Applied Physics* 43, 124002 (2010).
32. D.R. Demers and C.D. Allemand, *Analytical Chemistry* 53, 1915 (1981).
33. J.F. Waymouth and F. Bitter, *Journal of Applied Physics* 27, 122 (1956).
34. T. Jüstel, J.-C. Krupa, and D.U. Wiechert, *Journal of Luminescence* 93, 179 (2001).
35. H. Kim, *Plasma Processes and Polymers* 1, 91 (2004).
36. M.A. Malik, A. Ghaffar, and S.A. Malik, *Plasma Sources Science and Technology* 10, 82 (2001).
37. A. Bogaerts, E. Neyts, R. Gijbels, and J. van der Mullen, *Spectrochimica Acta Part B: Atomic Spectroscopy* 57, 609 (2002).
38. M.G. Kong, G. Kroesen, G. Morfill, T. Nosenko, T. Shimizu, J. van Dijk, and J.L. Zimmermann, *New Journal of Physics* 11, 115012 (2009).
39. G.E. Morfill, T. Shimizu, B. Steffes, and H.-U. Schmidt, *New Journal of Physics* 11, 115019 (2009).
40. X. Lu, Y. Cao, P. Yang, Q. Xiong, Z. Xiong, Y. Xian, and Y. Pan, *IEEE Transactions on Plasma Science* 37, 668 (2009).

2

Atmospheric Pressure Plasmas

Peter J. Bruggeman

2.1 Introduction

Atmospheric pressure plasmas (APPs) are very diverse and have widespread applications such as in waste reduction and gas purification, chemical conversion and syntheses such as ozone production, nanoparticle synthesis, surface functionalization of materials, and disinfection.

It is relatively easy to produce nonequilibrium* gas discharges at low pressure with gas temperatures close to room temperature. With increasing pressure, however, gas discharges have the tendency to become unstable and constricted: typically a glow-to-spark/arc transition occurs. At atmospheric pressure it is thus necessary to use special geometries, electrodes, or excitation methods to obtain nonequilibrium plasmas for which the gas temperature remains significantly smaller than the electron temperature.

In this chapter a description of the basic properties of different APPs is given. We start with a discussion on energy transfer and heating in APPs, which have direct implications for the wide range of gas temperatures occurring in APPs. Next the typical timescales of important chemical and physical processes are presented. High-pressure (atmospheric pressure) discharges also have some specific chemical and physical properties that differ from those of low-pressure discharges, which are outlined

* In the case of a nonequilibrium discharge the electron temperature (T_e) is significant larger than the gas temperature (T_g).

in a separate section. This is followed by a discussion on the electrical breakdown at atmospheric pressure and by transitions and instabilities of high-pressure plasmas. The different APPs are classified according to the excitation method and/or geometry. First DC and low-frequency AC capacitively coupled discharges that often have a high gas temperature and can even be in local thermal equilibrium (LTE), for which $T_e = T_g$, are discussed. The same can be said for inductively coupled plasmas (ICPs) and microwave (MW)-excited plasmas. All other discharge types are used when one of the goals is to reduce gas heating as much as possible. These discharges include corona discharges, radiofrequency (RF) and pulsed glow discharges, dielectric barrier discharges (DBDs), and so-called microplasmas.

It is not the goal to address all the specific topics in detail but rather to discuss and illustrate the general working mechanisms of APPs. More details on specific topics can be found in the dedicated chapters in this book or in references provided in the text.

2.2 Energy Transfer and Heating: Fundamental Relations

As most APPs are produced by applying a voltage across two electrodes, the electrical energy that is contained in the electric field in the electrode gap is transferred to the plasma by accelerating charged species. In general at high pressure there is limited direct energy transfer of the electric field to the heavy particles (ions) and the electrons are mainly heated by the electric field. The energy transfer of the electrons to the heavy particles (gas molecules) occurs through ionization, excitation, dissociation of molecules, and elastic collisions. In many steady-state high-pressure discharges the electron temperature is between 1 and 3 eV, and in this case, in atomic gases, the energy transfer from the electrons to the heavy particles is mainly dominated by elastic collisions. In the case of molecular gases vibrational excitation is normally dominant in this range of electron temperatures. An example of the relative energy transfer from electrons to the different processes is shown in the case of Ar and N_2 in Figure 2.1. Note that the energy transfer from the electric field to the electrons can be much more efficient than the subsequent collisional energy transfer between electrons and heavy particles mainly because only a fraction of about 10^{-4} of the energy difference between the electron and the heavy

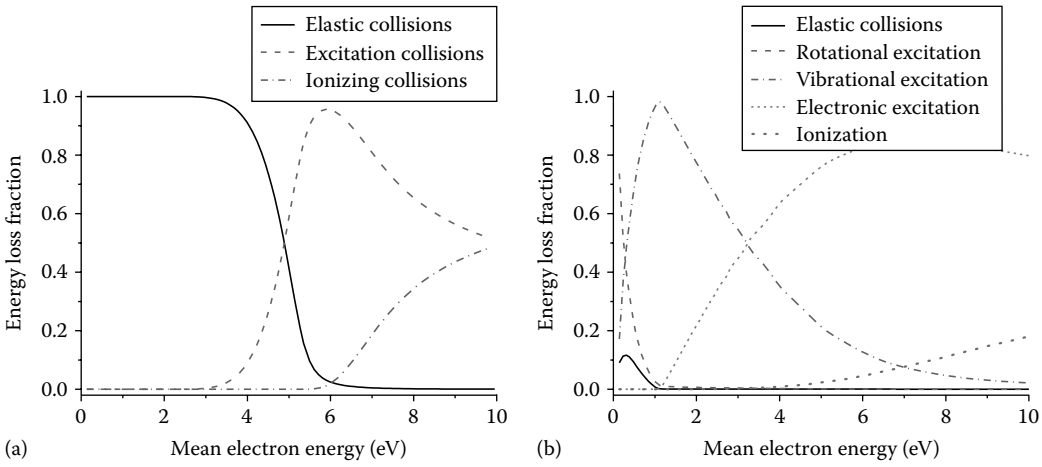

FIGURE 2.1 (a) Energy loss fractions of electron collisions in Ar consisting of elastic, excitation, and ionization collisions. (b) Energy loss fractions of electron collisions in N_2 consisting of elastic collisions, rotational, vibrational, electronic excitation, and ionization collisions. The data are obtained by the program Bolsig +. (Data from Hagelaar, G.J.M. and Pitchford, L.C., *Plasma Sources Sci. Technol.*, 14, 722–733, 2005.)

particle is transferred in each collision due to the large mass difference. Thus, the gas temperature can be significantly lower than the electron temperature.

Let us now consider a plasma in an atomic gas with an electron temperature below 3 eV. The energy transfer of the electrons to the gas by elastic collisions is determined by the elastic collision rate coefficient. Typical elastic collision rates are of the order of 10^{-13} m^3 s^{-1}. With increasing pressure, the collision frequency increases, which causes a more efficient energy transfer and thus gas heating. The difference between the electron temperature and gas temperature can be estimated by equating the average energy gained by an electron in the electric field between two collisions and the average energy transferred in a collision between an electron and a neutral. This leads to the following equation (Finkelnburg and Maecker 1956):

$$\frac{T_e - T_g}{T_e} = \frac{m_g}{4m_e} \frac{\left(\lambda_e e E\right)^2}{\left(\frac{3}{2} k_B T_e\right)^2}, \tag{2.1}$$

where

m_g is the heavy neutral particle mass
m_e is the electron mass
k_B is the Boltzmann constant
E is the electric field
e is the elementary charge
λ_e is the electron mean free path

Equation 2.1 shows that the difference between T_e and T_g increases with increasing pressure (decreasing main free path) and increasing electric field. Figure 2.2 illustrates a typical pressure dependence of T_e and T_g for a steady-state arc plasma. Of course the dependence in this figure is only valid when the gas temperature is mainly determined by the balance between the electron energy transfer to the heavy particles and not by strong heat removal which, for example, occurs in regions of large plasma gradients such as sheath regions or when a strong gas flow is applied.

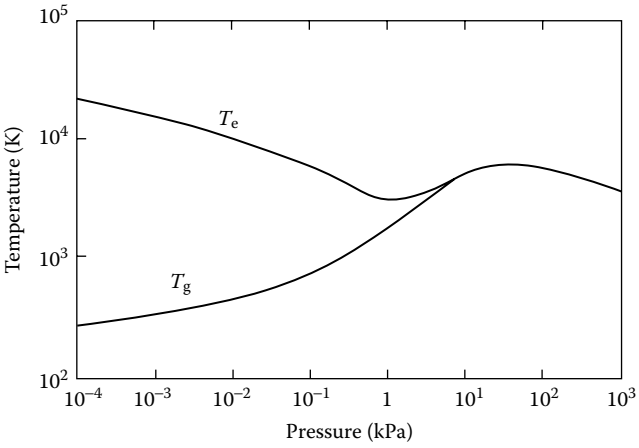

FIGURE 2.2 Electron temperature and gas temperature in a mercury arc as a function of pressure. (Reprinted from *Gaseous Electronics: Electrical Discharges*, 1, Hirsh, M.N. and Oskam, H.J., Electric arcs and arc gas heaters, 291–398, Copyright 1978, with permission from Elsevier.)

A lot of additional insight can be obtained from a power balance between the energy input in a plasma and the heat removal. Assuming that the energy used per ionization in the bulk is known and equal to $E(T_e)$,* the power dissipation in the plasma can be written as

$$\frac{P_{heat}}{V} = n_e n_g k_e(T_e)\varepsilon(T_e),$$

where

n_e is the electron density
n_g is the neutral gas density
$k_e(T_e)$ is the (effective) ionization rate
P_{heat} is the power
V is the plasma volume

One can estimate the heat loss (P_{loss}) in the plasma as follows by assuming that the heat loss is mainly due to thermal conduction in the gas phase:

$$\frac{P_{loss}}{V} = -\nabla\lambda\nabla(T_g - T_{wall}) \propto \frac{n_g T_g^{3/2}}{L^2},$$

where λ is the thermal conductivity of the gas. On the right-hand side of the equation the gradient is estimated by a plasma dimension L, the wall temperature (T_{wall}) is assumed to be much smaller than T_g, and $\lambda \propto n_g\sqrt{T_g}$ as is known from kinetic gas theory. By assuming that the energy dissipation in the plasma equals the heat loss in the steady-state condition, the following relation can be deduced:

$$n_e L^2 \propto \frac{T_g^{3/2}}{\varepsilon(T_e)k_e(T_e)}. \tag{2.2}$$

This relation clearly shows that the gas temperature increases with increasing electron density and increasing plasma size. Low-density small-sized plasmas will thus always have a smaller T_g than their large-density large-sized counterparts.

Equations 2.1 and 2.2 show that to obtain nonthermal plasmas for which $T_e \gg T_g$, the following approaches can be used:

- Preventing thermalization/equilibrium by pulsing the plasma
- Increasing the electric field by using sharp electrodes as in corona discharges
- Reducing n_e or the current by introducing dielectric or resistive barriers
- Improving the heat transfer by
  - Forced convection
  - Using gases with a large thermal conductivity such as helium
  - Reducing the plasma size

It is important to note that plasmas produced by continuous DC excitation that have a relatively large volume at atmospheric pressure often have an elevated T_g that can approach T_e. The most natural high-pressure plasma is thus a hot plasma, and to obtain plasmas that operate close to room temperature one or more of the approaches summarized above can be employed.

2.3 Typical Timescales

The different physical and chemical processes that are of importance or directly influence the plasma properties at atmospheric pressure span a time range of about 12 orders of magnitude. It is thus very important to have a good understanding of which processes are relevant especially for time-modulated plasmas.

* In this energy the average energy losses by all elastic and inelastic collisions are included. For more details the reader is referred to Lieberman (2005).

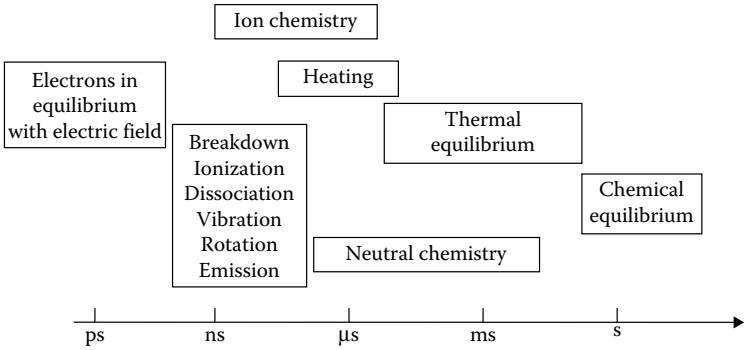

FIGURE 2.3 Schematic overview of the typical important timescales in APPs.

An overview of the most important physical and chemical processes is shown in Figure 2.3. The fastest timescale is of the order of picoseconds and determines the equilibrium of the electrons in the applied electric field. The typical neutral collision frequency at atmospheric pressure is of the order of 10^9 s^{-1} at room temperature. Ionization typically occurs at nanosecond timescales. Heavy particle heating takes a significantly longer time, that is, about 100 ns–1 μs. For chemical reactions (e.g., radical formation) three different timescales need to be considered: (1) electron-induced dissociation reactions for larger T_e values typically occurs on timescales of a few nanoseconds; (2) radical chemistry due to interaction with neutrals is mainly on a microsecond timescale; and (3) ionic reactions that are important in higher density plasmas occur at an intermediate timescale, which is typically in the range 10 ns–1 μs.

It normally takes several milliseconds for thermalization to occur between the electron and gas temperature. As thermalization is a necessary condition for chemical equilibrium it only occurs at a timescale of seconds. The above-mentioned timescales are the reason why plasma chemistry is in most cases strongly nonequilibrium chemistry. Note that reaction rates can strongly depend on T_e and n_e, so different plasmas can have different timescales for ionic and electronic processes.

2.4 High-Pressure Plasma Chemistry

As we have seen above, at low pressure the (elastic) collision frequency is much smaller compared to that at atmospheric pressure. Apart from an increase in collision frequency a shift in dominant chemical reactions can occur.

A very straightforward example is three-body reactions that are of increasing importance at high pressure. Two examples that are the basis of two major applications of atmospheric pressure are (Kogelschatz 2003):

ozone formation

$$O + O_2 + O_2 \rightarrow O_3 + O_2$$

and

excimer formation (e.g., in xenon)

$$Xe_m + 2Xe \rightarrow Xe_2^* + Xe,$$

in which the Xe_2^* decay causes the excimer band emission in the UV at around 172 nm. Both ozone generators and excimer lamps (and lasers) are based on high-pressure discharges because the above processes

are very slow at reduced pressures as the rate constant has a quadratic dependence with the gas density. Note that in general the heterogeneous (surface) reactions that often play an important role at low pressure become significantly less important at high pressure, and apart from a few exceptions bulk chemistry becomes dominant.

A second difference at atmospheric pressure is the ion chemistry. Even in the case of atomic noble gases, at high pressure and not very elevated temperatures atomic ions are quickly converted into molecular ions:

$$Ar^+ + 2Ar \rightarrow Ar_2^+ + Ar.$$

Typical rates of dissociative electron–ion recombination such as for the following reaction

$$e + Ar_2^+ \rightarrow Ar_m + Ar,$$

are of the order of 10^{13}–10^{14} $m^3\,s^{-1}$, which is several orders of magnitude faster compared to three-body electron–ion recombination or radiative electron–ion recombination for which a second electron or photon is necessary to simultaneously conserve momentum and energy (Fridman 2009):

$$Ar^+ + 2e \rightarrow 2Ar + e \quad \left[k \approx 10^{-39}\ m^6 s^{-1}\ (T_e = 1\ eV)\right],$$

$$Ar^+ + e \rightarrow Ar + h\nu \quad \left[k \approx 3 \times 10^{-19}\ m^3 s^{-1}\ (T_e = 1\ eV)\right].$$

Because of the low recombination rates of atomic ions in low-pressure plasmas, diffusion is often the dominant particle-loss mechanism, while at atmospheric pressure (for which the electron density is often in the range of 10^{20}–10^{21} m^{-3}) dissociative electron–ion recombination and thus bulk recombination often becomes dominant compared to wall losses. Additionally, at high pressure dissociative recombination and in general ion chemistry can play an important role in radical production when the ion density is significantly large (10^{20}–10^{21} m^{-3} or larger). A typical example is OH production on the edge of a plasma filament, which can be explained by charge exchange and dissociative electron–ion recombination reactions when the core of the filament is assumed to consist mainly of atomic ions and the water is fully ionized (Verreycken et al. 2012):

$$H^+ + H_2O \rightarrow H_2O^+ + H \quad (k \approx 7 \times 10^{-15}\ m^3 s^{-1}),$$

$$H_2O^+ + H_2O \rightarrow H_3O^+ + OH \quad (k \approx 10^{-15}\ m^3 s^{-1}),$$

$$H_3O^+ + e \rightarrow OH + 2H \quad \left[k \approx 10^{-13}\ m^3 s^{-1}\ (T_e = 1\ eV)\right].$$

In electronegative gases, negative ion chemistry can be significantly different at high-pressure compared to low-pressure plasmas. At low pressure attachment mainly proceeds through dissociation, which requires bridging the threshold energy for the dissociation. A typical example is

$$O_2 + e \rightarrow O + O^-.$$

However, at atmospheric pressure three-body attachment plays a key role for balancing the charged particles

$$O_2 + e + M \rightarrow O_2^- + M,$$

where M is a third-body heavy particle. This is particularly important for pulsed discharges in air for which the above three-body attachment reaction is often a dominant charge-loss mechanism in the recombination phase, because of which when the next pulse is applied negative ions can increase the production of electrons in the newly developing ionization front. For a more detailed discussion on ion chemistry in APPs, the reader is referred to the book *Plasma Chemistry* (Fridman 2009).

An additional difference at high pressure compared to at low pressure is the strong electronic quenching of excited states, which in some cases significantly reduces the emission. Many examples

exist such as for the excited OH(A), which causes the typical OH(A–X) emission band at around 306 nm. The excited state can be strongly quenched (and correspondingly the emission drastically reduced) due to the competitive reaction

$$\mathrm{OH(A)} + \mathrm{M} \rightarrow \mathrm{OH(X)} + \mathrm{M}^{*},$$

where M is a colliding heavy particle. This phenomenon not only plays an important role in applications such as in the production of efficient gas discharge lamps but is also of importance for fundamental investigations and diagnostics when probing the OH density by laser-induced fluorescence.

2.5 Breakdown, Transitions, Instabilities, Constrictions, and Streamer Formation

A typical figure that is discussed in almost every textbook is the current–voltage (*I–V*) characteristic of a DC discharge in a range from nanoamperes up to several kiloamperes, as shown in Figure 2.4. The graph is of course not stably realizable in one single setup, but it illustrates the different stages of a discharge. Basically when a voltage is applied to the electrodes, the charges produced by external influences (cosmic radiation and so on) are collected at the electrodes. At some value of the voltage the electric field is large enough to accelerate electrons, which can cause ionizing collisions. This process continues with the help of secondary electron emission at the cathode and develops into a Townsend discharge for which the space charge is still negligible. With increasing current, space charge becomes important and sheaths are formed at the electrode so a transition to a glow discharge occurs. This transition is often called a breakdown as a glow discharge is a self-sustained discharge. With a further increase in current, the current density starts to increase when the transition from a normal glow to an abnormal glow occurs and plasma heating becomes important. At a critical point this triggers a transition to an arc discharge.

At low pressure, a common breakdown mechanism is the Townsend breakdown. Basically avalanches run between two metal electrodes in a homogeneous applied field, and space charge effects are negligible. During this process the electron density builds up by bulk ionization, and secondary electron emission occurs by ionic impact at the cathode (Figure 2.5a). However, with increasing pressure ionization can occur on much smaller length scales, and space charge effects are sometimes no longer negligible.

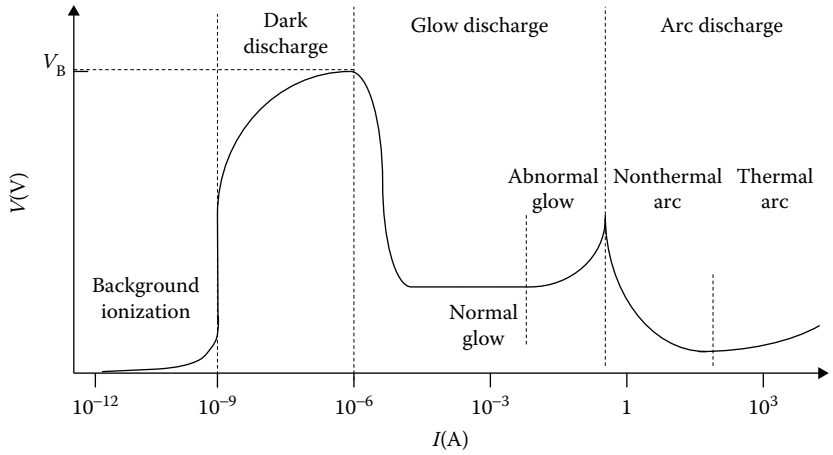

FIGURE 2.4 *I–V* characteristic of a parallel-plate discharge and the transitions from Townsend to glow and arc discharge. (Modified from Roth, J.R., *Industrial Plasma Engineering*, Institute of Physics Publishing, Bristol and Philadelphia, 1995.)

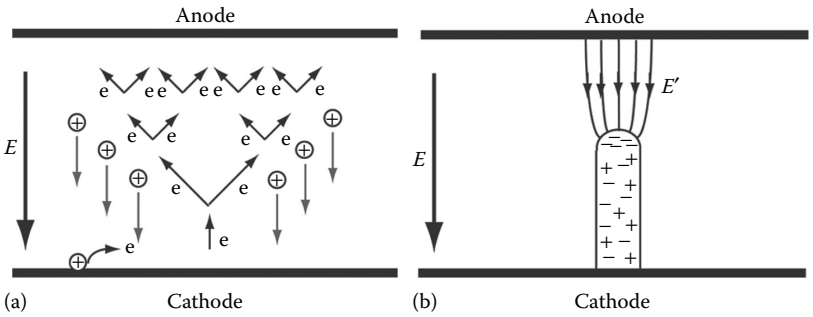

FIGURE 2.5 Schematic representation of (a) Townsend breakdown and (b) streamer breakdown.

The amount of charge in the gap can, at sufficient charge density, produce its own electric field that equals the applied homogeneous electric field, and it can effectively sustain its own ionization front and a transition to a filamentary self-propagating ionization front which is called a streamer occurs (Figure 2.5b). The criterion for the conditions under which the transition to a streamer occurs is called the Meek criterion. In the case of air at atmospheric pressure the criterion can be estimated as follows (Raizer 1987):

$$\int_0^d \left[\alpha\left(\frac{E}{N}\right) - \beta\left(\frac{E}{N}\right) \right] dx \approx 18 - 20, \tag{2.3}$$

where

α is the Townsend ionization coefficient
β is the attachment coefficient
E/N is the reduced electric field
d is the gap length

Note that from this criterion a critical electron density can also be estimated, which is of the order of 10^{17} m^{-3} in the case of air at atmospheric pressure. When the Meek criterion is satisfied, the Townsend discharge changes into a streamer, which can subsequently change into a spark when reaching the second electrode. In the spark significant gas heating occurs, and depending on the power input of the power supply it turns into an arc- or a glow-like discharge and even quench.

If a diffuse discharge is required, one needs to ensure that the Meek criterion is not reached. Apart from obvious techniques such as varying the geometry and excitation voltages, streamer formation can be prevented by preionization and slowing down the ionization in the avalanche by using well-chosen gas mixtures that strongly influence the ionization process.

The approach of using preionization is perhaps not self explaining but is relative easy to understand (Levatter and Liu 1980). Two avalanches that are close to each other are impacted by each other's electric field. The electric field of these avalanches is the same but has a different sign in the overlapping region of the field lines. This causes an effective reduction of the electric field in the avalanche. Increasing the preionization will increase the number of avalanches in the discharge gap, and thus the average distance between the avalanches is reduced so the electric field buildup by one avalanche is reduced by the surrounding avalanches. Reducing the electric field and thus the ionization frequency directly reduces the integral in Equation 2.3 and ensures that the Meek criterion is not fulfilled and the avalanche to streamer transition is postponed.

Another more chemical approach is introducing a two-step ionization such as Penning ionization:

$$Ar_m + M \rightarrow Ar + M^+.$$

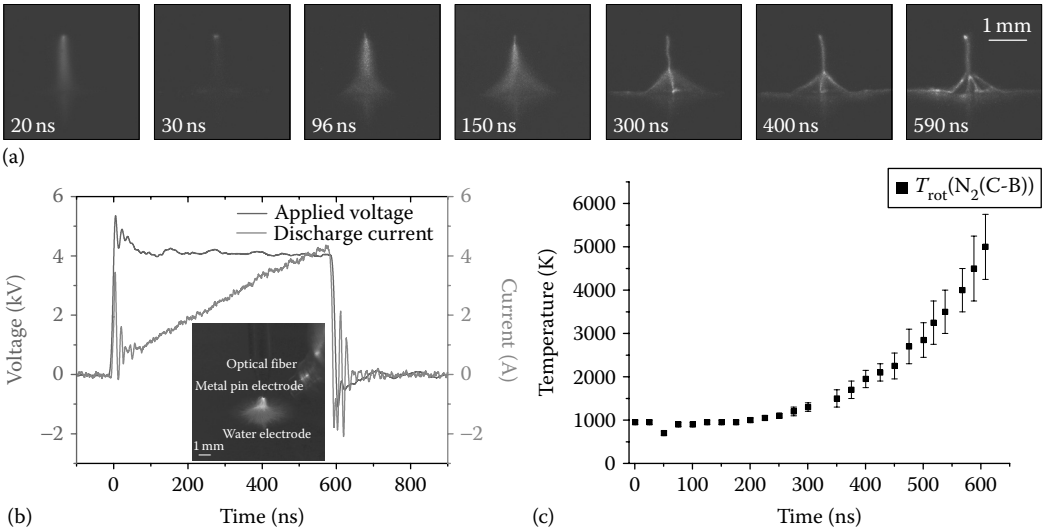

FIGURE 2.6 (a) 10 ns resolved images of a 600-ns pulsed discharge in air between a metal pin electrode and a water surface. (b) The corresponding *I–V* waveform. A time-averaged image (integration time of 1/30 s) of the plasma is inserted in the graph. (c) The evolution of the gas temperature during the plasma pulse. The constriction of the discharge around 300 ns can be clearly seen with a corresponding temperature increase. (Reprinted with permission from Bruggeman, P., et al., *Plasma Sources Sci. Technol.*, 18, 045023, 2009, © IOP.)

Basically one adds a trace gas to the bulk gas (e.g., Ar). The production of Ar metastables (11 eV) can be done at smaller electric fields compared to the ionization of Ar (15.6 eV). The metastables then easily ionize molecules or atoms (M) with an ionization energy ≤11 eV, and if this Penning ionization is the dominant mechanism, then the two-step process is typically slower than a direct ionization and can proceed at smaller electric fields. An example is the generation of Ar discharges with a trace gas such as ammonia, which is diffuse for conditions for which a pure Ar discharge is filamentary (Massines et al. 2009).

In order to understand the typical timescales of glow-to-spark/arc transition, it is illustrative to discuss the example of a DC pulsed discharge, as shown in Figure 2.6. The discharge is produced by applying a 600 ns voltage pulse (with amplitude of 4 kV) to a needle electrode positioned 1.5 mm above a water surface that serves as a grounded electrode. The plasma is operated in air (containing water vapor evaporated from the liquid water electrode) at a frequency of 6 kHz. From Figure 2.6 it is clear that a transition occurs at 300 ns when the plasma constricts. This constriction coincides with the start of a close to exponential increase in the gas temperature. The exact timescale of the increase depends on the specific conditions (applied voltage, energy injected in the discharge, electrode material, etc.) but a typical timescale for excessive heating is of the order of 100 ns. It shows that pulsing the plasma to prevent instabilities (contraction) from occurring has to be done at typical timescales of 10–100 ns.

The above example also clearly illustrates the tendency of APPs to constrict and not be diffuse but rather filamentary. This is generally valid as can also be seen in naturally occurring plasmas such as the aurora high in the atmosphere (at low pressure), which is diffuse, and lightning close to the earth's surface at atmospheric pressure, which is strongly filamentary.

A constriction of an initially diffuse (glow) discharge is a common instability. This instability is induced and coincides with an increase in electron density and gas temperature. When a discharge is stable, electron production is balanced by electron losses. The electron density demonstrates runaway behavior if the plasma operates under conditions such that an increase in the

electron density cannot be compensated by electron loss. Mathematically, the balance of the electron density can be written as

$$\frac{\mathrm{d}n_\mathrm{e}}{\mathrm{d}t} = k_\mathrm{ion}(T_\mathrm{e})n_\mathrm{e}n_\mathrm{g} - \frac{D_\mathrm{a}}{\Lambda^2}n_\mathrm{e} - k_\mathrm{dr}n_\mathrm{e}^2, \tag{2.4}$$

where

k_dr is the dissociative recombination losses
D_a is the ambipolar diffusion coefficient
Λ is the effective diffusion length

If a change in electron density does not influence the electron temperature, the ionization rate scales linear with n_e. Thus, diffusion and dissociative recombination contribute to stabilizing the discharge when a fluctuation of the ionization rate causes a small linear increase in n_e.

However, any process that increases the ionization rate faster than the linear dependence of n_e on the diffusion losses can cause potentially runaway behavior. This occurs with an increase in the gas temperature. Indeed, an increase in the gas temperature leads to an increase in the reduced electric field (E/N) (assuming that the electric field remains constant as in the positive column of a glow discharge). This leads to a subsequent increase of the electron temperature and ionization rate, which increases the electron density. A larger electron density in turn leads to more Ohmic losses and thus an increase in gas temperature. It is clear that this process causes an increase in the ionization rate in Equation 2.4 and causes a stronger effective dependence on the electron density than the linear dependence when T_e remains constant. The heating and increase in T_e preferentially happen in the core of the discharge, which also promotes the radial shrinking of the discharge. The above instability is referred to as thermal instability and is common in high-pressure gas discharges.

Apart from thermal instability, stepwise ionization due to a stronger accumulation of metastable species can significantly increase the ionization rate and also cause instabilities. This is why in some cases strong gas flow is used to stabilize the discharge. An additional instability can also be triggered in electronegative discharges when detachment (which is independent of T_e) balances a significant part of the attachment. In this case an increase in n_e will lead to a reduction in T_e and consequently a reduction in the attachment rate. In this case the detachment is faster compared to the effect of gas composition on the attachment, and the detachment causes a further increase in n_e.

An example of constriction of a high-pressure atomic plasma column is studied by Castaños-Martínez et al. (2009) for an atmospheric pressure MW discharge in Ar–Ne mixtures. It has been shown that both pure Ne and Ar discharges are radially constricted, while a Ne discharge with an addition of 0.5–1% Ar fills the entire tube and is more diffuse (Figure 2.7). Note that the ionization energy of Ne and Ar is 21.6 eV and 15.6 eV, respectively. The charge conservation in the case of an Ar discharge with Ar_2^+ as the dominant ion is governed by the following reactions:

$$\mathrm{e} + \mathrm{Ar}_2^+ \rightarrow \mathrm{Ar}_\mathrm{m} + \mathrm{Ar},$$

$$\mathrm{e} + \mathrm{Ar}_\mathrm{m} \rightarrow \mathrm{Ar}^+ + 2\mathrm{e},$$

$$\mathrm{Ar}^+ + 2\mathrm{Ar} \rightarrow \mathrm{Ar}_2^+ + \mathrm{Ar}.$$

Note that in this case the ionization is very fast and depends nonlinearly on the electron density as the electron loss process produces metastables that can easily be ionized (energy threshold of about 4 eV) in a plasma with a T_e of 1–2 eV (which is typical for these MW discharges). The ionic and electronic losses are also bulk losses and not determined by diffusion.

In the case of the diffuse plasma, however, the dominant ion is Ar^+ and the following reactions dominate the charge balance:

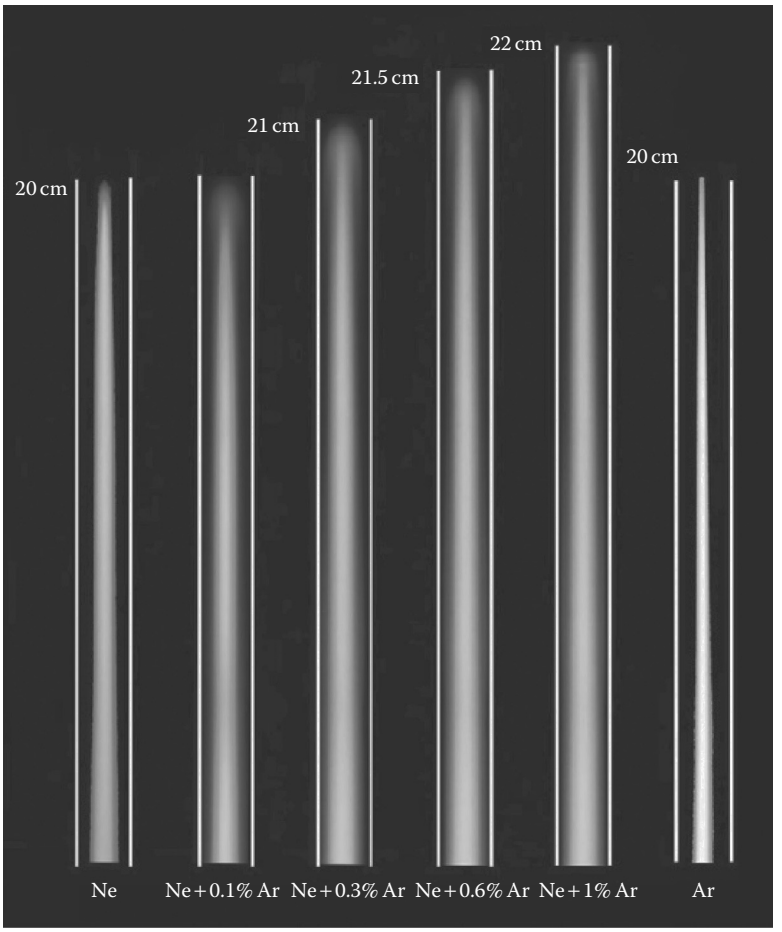

FIGURE 2.7 Images of a surface wave tubular discharge in Ne–Ar mixtures at atmospheric pressure. The diameter of the dielectric tube (indicated in the image by the white lines) is 12 mm. Both the pure Ne and Ar discharges are contracted but a mixture of Ne with about 1% of Ar fills the entire tube with a diffuse discharge. (Reprinted with permission from Castaños-Martínez, E., et al., *J. Phys. D Appl. Phys*., 42, 012003, 2009, © IOP.)

$$e + Ar \rightarrow Ar^{+} + 2e,$$

$$e + Ne \rightarrow Ne_{m} + e,$$

$$Ne_{m} + Ar \rightarrow Ar^{+} + Ne,$$

$$e + Ar^{+}\,(+Ar) \rightarrow Ar\,(+Ar).$$

The ionization rate is clearly much smaller as it is dominated by Penning ionization and direct electron ionization from the ground state of Ar. This is consistent with the above discussion on ionization instabilities. Additionally, the recombination rate of atomic ions is about 5 orders of magnitude smaller than the dissociative recombination rate, which makes ambipolar diffusion the dominant loss mechanism for charged species in this diffuse discharge.

Note that the above mechanism seemingly has similarities with the Penning mixtures used to create diffuse discharges and prevent streamer formation. However, it is important to realize that in high-density

diffuse discharges, processes at timescales that are significantly slower compared to the few nanoseconds in which an avalanche crosses the electrode gap can be important for ionization. The charge density is also significantly larger; thus recombination products from the produced ions can indeed facilitate the charge creation, while this is not the case in an ionization front.

The above case is a typical example of APP instabilities. In several discharges that are contracted dissociative recombination is the dominant loss mechanism. This is mainly due to the fact that atomic ion recombination is normally significantly slower and in this case ambipolar diffusion is often important, which also causes the discharge to become more diffuse. The above illustrates that a requirement for contraction is that the electrons or ions have to be produced and lost locally. This can be important even in atomic noble gases for which the dominant ion can be a dimer (e.g., Ar_2^+).

2.6 DC and Low-Frequency AC Capacitively Coupled Discharges

2.6.1 DC and Low-Frequency AC-Excited Glow Discharges

The classical low-pressure glow discharge has been studied extensively for several decades. The light emission pattern of a low-pressure glow discharge is described in most standard gas discharge textbooks and includes a cathode glow, a cathode dark space, a negative glow, Faraday dark space, a positive column, an anode dark space, and an anode glow (e.g., Lieberman and Lichtenberg 2005). The main characteristic of the DC glow discharge is that the discharge is maintained by electron production at the cathode by secondary electron emission due to ion impact. At high pressure ionization in the sheath also occurs. The electrons originating from the cathode are accelerated in the sheath and cause significant ionization, which maintains the discharge. The positive column just connects both sheath regions. The constant electric field in the positive column ensures that the electron losses are compensated by an equal amount of electron production.

In spite of the fact that it is easy to produce DC glow discharges at low pressure, with increasing pressure the glow discharge has the tendency to become unstable and constricted: a glow-to-arc/spark transition then occurs. At atmospheric pressure it is thus necessary to use special geometries, electrodes, or excitation methods to obtain diffuse glow discharges. As the timescale on which a glow-to-arc/spark transition occurs is typically of the order of (a few) 100 ns (see previous section), switching off the discharge before the transition to a spark/arc occurs is an often used approached to produce diffuse atmospheric pressure glow discharges. A lot of studies on the glow-to-spark transition are reported. Unfortunately, the instability (constriction) can occur in the cathode, the anode, and the positive column region. This illustrates that the exact discharge geometry, electrode properties, and even gas composition have a strong influence on the instabilities of the glow discharge. Nonetheless, there needs to be a minimum power input for the glow-to-spark transition to occur. This is related to a large electron density and an increase in the gas temperature, conditions under which thermal instability can occur.

In some literature the term glow discharges is used for a diffuse-looking discharge. However, even diffuse-looking atmospheric pressure discharges can consist of a large number of filaments. It is therefore more correct to reserve the term glow discharge for a discharge with properties similar to those of a glow discharge at low pressure.

The typical properties of a normal glow discharge that are also valid at atmospheric pressure include the following:

- The reduced current density (J/N) is independent of the density and applied voltage.
- The characteristic light emission pattern, especially the cathode dark space, is visible, although the size is significantly smaller compared to the low-pressure cases as it scales with density.
- The discharge voltage is independent of the current when corrected for temperature rise, constriction of the positive column, and current dependence of the cathode–anode voltage drop.
- The burning voltage and cathode voltage drop is significantly larger than for an arc discharge.

Nonetheless, apart from the similarities with low-pressure glow discharges, there are several differences. The electron temperature is still significantly larger compared to the gas temperature, but due to the higher pressure the collisionallity is much larger and the gas temperature can reach 1000 K or more in a glow discharge. Therefore, the typical scaling laws valid at low pressure have to be used as a function of density and not pressure.

Additionally, the sheath is highly collisional at atmospheric pressure, which means that the ion energies impacting on the electrode or substrate are significantly lower (typically not more than a few electron volts under standard conditions) compared to lower-pressure discharges, which can have ion energies of several tens of electron volts and are often used for material sputtering applications.

Diffuse atmospheric pressure glow discharges have an electron density in the range 10^{16}–10^{19} m^{-3} (e.g., Barinov et al. 1998). The main difference between low-pressure and atmospheric pressure glow discharges is the loss mechanisms for electrons in the positive column. At low pressure the electron losses are due to radial ambipolar diffusion, while at higher pressure electron–ion dissociative recombination becomes more important. Because of this difference in electron loss mechanisms, at larger electron densities/powers atmospheric pressure glow discharges are often contracted and resemble arc discharges. In electronegative gases such as air, attachment losses can be important.

A recent study of the glow-to-spark transition in a metal pin–water electrode geometry showed that broadened sparks occur close to the water electrode (Bruggeman et al. 2008b). This illustrates the stabilizing effect of resistive (water) electrodes on the constriction of diffuse glow discharges even after a contraction has occurred in the bulk of the discharge. Stable DC and low-frequency AC-excited glow discharges in air at atmospheric pressure have been obtained by Laroussi et al. (2003) by using liquid electrodes. An example of a DC-excited glow discharge at atmospheric pressure with a liquid electrode that clearly illustrates the different characteristic zones of a glow discharge is shown in Figure 2.8.

A second approach to stabilize DC or low-frequency AC-excited glow discharges is by applying a fast gas flow. Significant gas flow not only can hasten heat removal in the discharge but also can contribute in enhancing charge and radical transport, which additionally alter the discharge properties. Stable DC glow discharges have also been produced at atmospheric pressure between two metal electrodes in microgaps (Staack et al. 2007).

The term abnormal glow discharge is normally used for glow discharges that show an increase in voltage with increasing current. At low pressure this occurs when the current density increases in the case that the electrode area of the cathode is fully covered by the discharge. At high pressure the radial

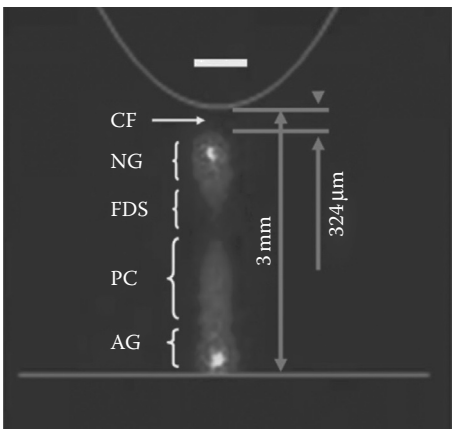

FIGURE 2.8 Glow discharge at atmospheric pressure between a metal pin cathode and water anode. The glow discharge is sustained at 1.25 mA and 1 kV. The structure of a glow discharge is clearly visible. CF, cathode fall; NG, negative glow; FDS, Faraday dark space; PC, positive column; AG, anode glow. (Reprinted with permission from Bruggeman, P., et al., *Plasma Sources Sci. Technol.*, 17, 045014b, 2008a, © IOP.)

diameter of the glow discharge is less and this specific phenomenon is mainly an issue when dealing with small electrodes.

2.6.2 Arc Discharges

The main difference between an arc and a glow discharge at atmospheric pressure is that the current of an arc is significantly larger (1 up to several kA) and the cathode sheath region is significantly different. Unlike in glow discharges in which the secondary electrons from the cathode are produced by ion impact, the secondary electron emission in arc discharges can be triggered by both thermal emission and field emission. As such, the cathode voltage drop is smaller (typically 15 V) because there is no need to accelerate the ions toward the cathode and the voltage drop only serves to accelerate the electrons up to the ionization threshold of the gas. Thermal emission of electrons can be calculated from the well-known Richardson equation for current density J (e.g., Boulos et al. 1994):

$$J = AT^2 \exp\left(-\frac{e\varphi}{k_B T}\right)(\mathrm{A\,m^{-2}}),$$

where the theoretical value of the constant A is equal to 1.2×10^6 A m^{-2}K^{-2}. However, the practical value of A depends on the electrode metal. As the work function φ is typically between 2 and 5 eV, thermal electron emission becomes important only at elevated temperatures typically present in an arc discharge.

The bulk region of an arc consists of a positive column that is normally more contracted than its counterpart in the glow discharge and also has a significantly higher electron density of 10^{22}–10^{25} m^{-3}. Arc discharges are typically categorized as thermal and nonthermal arcs. Low-pressure arc discharges are often nonthermal, as can be clearly seen in the steady-state T_e–T_g variation with pressure in Figure 2.2. In the case of thermal arcs it is often a significant simplification to assume that local thermodynamic equilibrium (LTE) exists. LTE conditions require that the following three conditions are fulfilled locally:

1. The velocity distributions of particles follow a Maxwell–Boltzmann distribution.
2. The population density of excited states follows a Boltzmann distribution.
3. The particle densities and ionization degrees follow the Saha equation.

The above three requirements are met when collision processes (and not radiative processes) govern transitions and reactions in plasma. Additionally, as mentioned, the gradients in plasma properties should be small, or, more accurately, the diffusion time should be larger than the time necessary to obtain equilibrium.

It is instructive to treat the third condition in more detail. The Saha equation (e.g., Boulos et al. 1994) is as follows:

$$\frac{n_i n_e}{n_a} = \frac{g_i g_e}{g_a}\left(\frac{2\pi m_e k_B T}{h^2}\right)^{3/2} \exp\left(-\frac{E_{ion}}{k_B T}\right),$$

where

E_{ion} is the ionization energy
h is the Planck constant
g and n are the degeneracy and densities of the ion, electron, and atom, respectively

This equation is obtained from the following reaction by assuming equilibrium

$$e + A \leftrightarrow A^+ + 2e,$$

and is a specific form of detailed balancing or a mass action law that can also be applicable for the dissociation degree in a molecular plasma. However, in the case of ionization, electron impact ionization

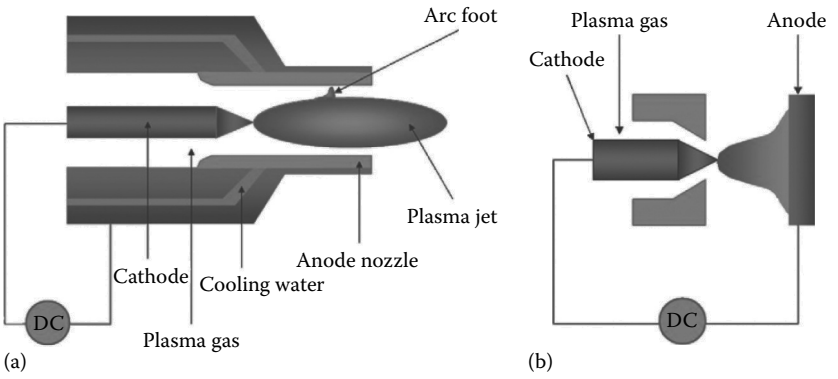

FIGURE 2.9 Schematic representation of (a) transferred arc and (b) nontransferred arc. (Reprinted from *Spectrochim. Acta Part B At. Spectrosc.*, 61, Tendero, C., et al., Atmospheric pressure plasmas: A review, 2–30, Copyright 2006, with permission from Elsevier.)

needs to be balanced by two electron recombinations. Thus, this equation is not applicable when molecular ions are present in the plasma or at low electron densities when other recombination losses such as dissociative molecular ion dissociation or diffusive losses are dominant.

In the context of applications one often refers to transferred and nontransferred arcs. In the case of transferred arcs, the arc is drawn between an electrode and a conducting workpiece. The energy transfer efficiency to the workpiece is very high, and the discharge has a large gas temperature. Transferred arcs are typically used in welding and cutting applications. Nontransferred arcs are basically remote plasma torches and are typically used for spraying and waste destruction. Many designs exist and the reader can refer to Boulos et al. (1994) and Roth (1995) for a more extensive overview. Two typical examples of a transferred and a nontransferred arc are shown in Figure 2.9.

It is important to remember that arc discharges have to be ignited with an additional voltage apart from the standard power supply. From Figure 2.4 it is clear that the discharge has to pass all the discharge stages that require a significantly larger voltage compared to that for an arc discharge. Often an arc is drawn by making contact with the two electrodes, or an inductor is used to produce a voltage spike as in a "lamp starter."

Arc discharges can also become unstable due to many prevalent phenomena. At currents of several kiloamperes and higher it is possible that the kinetic pressure of an arc column may not be able to withstand the inward magnetic pressure induced by the electric current through the column. In this case pinching occurs. This phenomenon can produce a very strong plasma that yields multiple ionized atomic ions and is used in applications for extreme UV generation (Kieft et al. 2003).

2.6.3 Gliding Arc Discharges

Gliding arcs have properties of both thermal and nonthermal plasmas. They are highly reactive and often have a high selectivity for chemical processes. The main reason why gliding arcs are often used for chemical-oriented studies is because they have properties of both thermal (large electron densities, currents, and power) and nonthermal plasmas (low gas temperature).

A gliding arc is normally generated between two diverging electrodes in a gas flow. An example of a configuration is shown in Figure 2.10.

The discharge ignites where the electric field is maximum, that is, at the smallest distance between the curved electrodes. This distance is typically of the order of a (few) millimeters. At this position a hot quasi-thermal plasma that moves upward is formed (due to the gas flow or the buoyancy force). As the electrodes are curved the length of the plasma column increases, increasing the heat losses in the column,

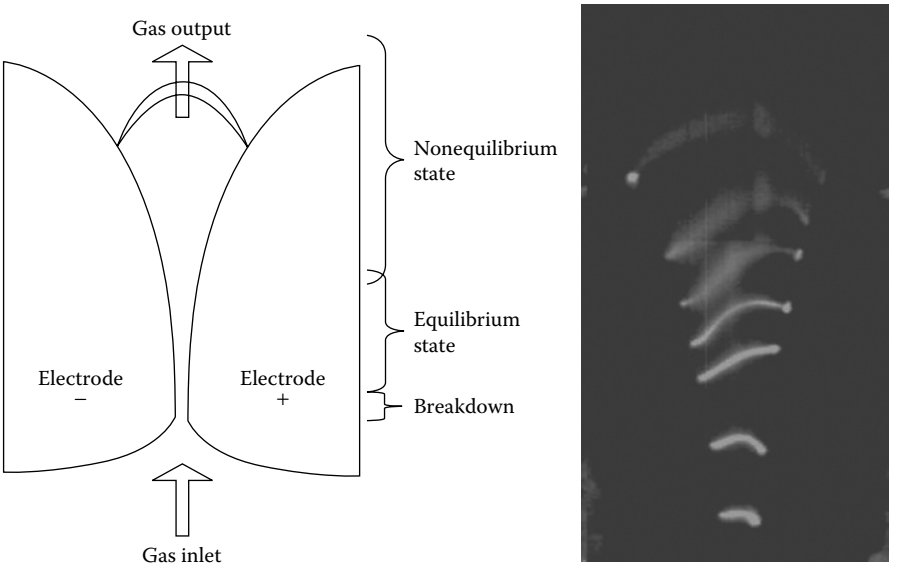

FIGURE 2.10 (a) Gliding arc electrode configuration with indication of the LTE and non-LTE region. (b) Superposition of snapshot images of a gliding arc discharge that illustrates the dynamic movement of the arc. (Reprinted with permission from Fridman, A., *Plasma Chemistry*, Cambridge University Press, Cambridge, 2008, © Cambridge University.)

which exceed the input energy of the power supply. Consequently, ionization reduces and quasi-thermal plasma is converted into nonthermal plasma. Eventually, the plasma extinguishes as the power supply cannot maintain such a long plasma column. Thereafter, recombination of plasma starts, and a reignition of the discharge occurs at the minimum distance between the electrodes. This self-pulsing nature is characteristic of a gliding arc discharge and typically occurs at a timescale of the order of 10 ms.

The exact plasma properties depend on the input power, which can range from about 100 W up to the order of 40 kW, corresponding to a gas temperature range from 2,500 K up to 10,000 K in the initial "quasi-thermal" state of the plasma. For the high power end, the gas temperatures in the nonthermal zone reduce to 1000–2000 K or even lower. The initial electron density is as high as in a typical arc, while the downstream or average electron density is of the order of 10^{17}–10^{19} m^{-3} (Kalra 2005).

The chemical efficiency of these discharges is due to the two distinctive phases in the plasma. In the thermal phase the molecules introduced in the discharge are strongly dissociated. The fast transition from a thermal to a nonthermal discharge (and a corresponding drop in the gas temperature) allows a fast recombination of the dissociation products to molecules and freezing of the reaction products, which are of key importance for applications requiring selective chemistry. As the flow is rather large it allows large throughputs with residence times of the reagents of the order of a millisecond. The above clearly illustrates why these discharges are typically used in applications related to chemical plasma conversion.

2.7 Inductively Coupled Plasmas

ICPs are used extensively at low pressure but can also operate at atmospheric pressure. They are often used as so-called analytical plasmas that ionize gases subjected to mass spectrometry (ICP-MS) or for spectroscopic analyses of trace components in gases and liquids. Also, ICPs are used for toxic gas/waste water treatment and coating applications. In an ICP the electrical power has a completely different coupling as compared to in a capacitively coupled plasma (see Figure 2.11). It basically consists of a helical

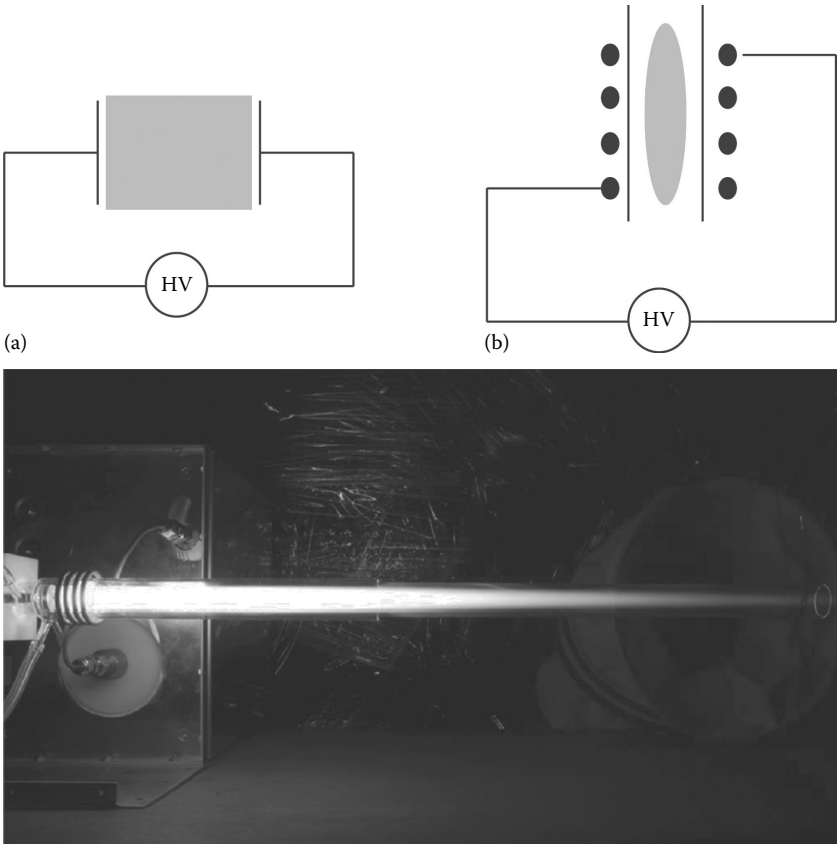

FIGURE 2.11 Comparison between a capacitively coupled discharge (a) and an inductively coupled discharge (b). (c) ICP discharge at atmospheric pressure operating at 1600 W in a mixture of N_2O, O_2, and air. The coil outside the tube produces the electric field inside the dielectric tube, which has an internal diameter of 16 mm. (Reprinted with permission from Tamura, T., et al., Direct decomposition of anesthetic gas exhaust using atmospheric pressure multigas inductively coupled plasma. *IEEE Trans. Plasma Sci*., 39, 1684–1688, © 2011 IEEE.)

coil wrapped around a dielectric tube in which the plasma is generated. By driving the coil with an RF field (typical in the megahertz range) the current in the coil induces a time-varying magnetic field in the tube, which causes a resulting electric field that accelerates the electrons and sustains the discharge. As ICPs are plasmas that are not directly in contact with electrodes or walls and no ionic sputtering of the wall occurs, they can be used for a large range of processing gases. Mostly they operate at high power (several kilowatts up to megawatts) and have a large electron density (10^{21} m^{-3} or larger) and a gas temperature close to the electron temperature (van de Sande et al. 2003). In the case of higher power the discharge is close to LTE, although for high flow rates, with the introduction of a liquid spray or low-power input, a stronger deviation from LTE can be found.

2.8 Wave-Heated Plasmas

Electromagnetic (EM) waves generated near a plasma surface can propagate into the plasma or along the surface and be absorbed by the plasma. EM waves can also lead to the ignition of a discharge when a local electric field that is high enough to cause breakdown is produced. The heating of the electrons in the plasma is caused by an EM wave. A typical example of wave-heated plasmas is the so-called

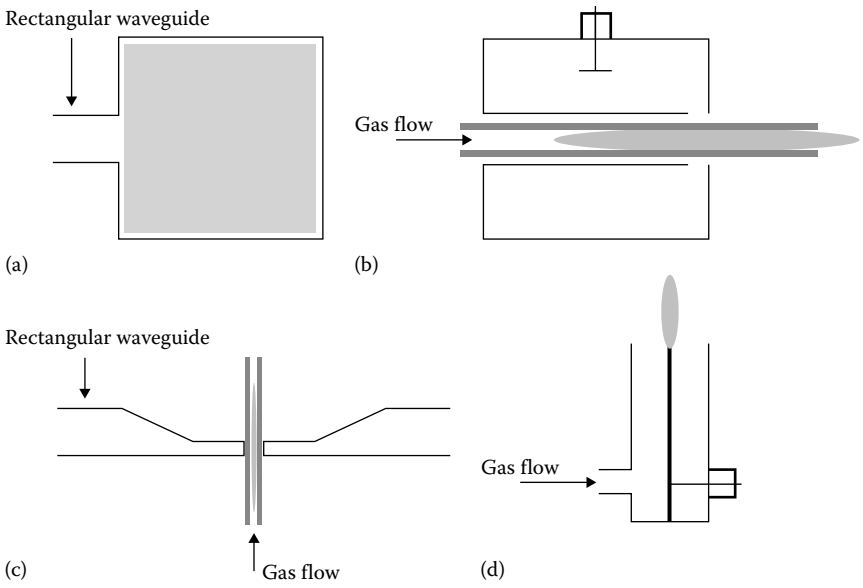

FIGURE 2.12 Four configurations that are commonly used to produce MW-excited discharges: (a) MW cavity, (b) surfatron, (c) surfaguide, and (d) antenna/electrode MW discharge. Many variations in geometries exist.

MW-excited plasma. Basically in the case of wave-heated plasmas one of the critical dimensions of the MW plasma should be comparable with the wavelength of the EM wave used for excitation, which implies that they should be generated at gigahertz frequencies. The coupling of MW power to the plasma can be done with different geometries based on different principles. An overview of four different geometries is shown in Figure 2.12. The conceptually easiest configuration is the MW cavity that is brought into resonance and the standing wave efficiently couples its energy into the plasma. As the geometry of the cavity and the plasma density determine the resonance frequency, the plasma is very sensitive to small changes in frequency (Figure 2.12a). The dependence of the resonance frequency on the plasma density confines application to a limited range of plasma conditions.

A second approach is using surface waves that travel along the plasma–dielectric boundary interface (Moisan and Zakrzewski 1991). Surface wave launching devices exist in different forms and can operate from frequencies below 1 MHz up to 40 GHz and more. It is based on the property that EM surface waves propagating along a cylindrical plasma column can be efficiently absorbed by the plasma, thus sustaining the plasma. A typical commonly used surface wave plasma device is the surfatron (see Figure 2.12b), which consists of a launcher cavity that has a small opening that allows the formation of a local high field in the dielectric tube. At this location ionization occurs and plasma is created. This plasma is then able to support a surface wave and it grows along the length of the column. This in turn creates specific conditions for long plasma columns. The surface wave attenuates due to the losses as it propagates along the plasma column, which causes a decrease in electron density with increasing distance from the launcher.

It is also possible to run a surface wave plasma in the gigahertz region by passing the dielectric discharge tube through the broad face of a waveguide (as shown in Figure 2.12c). Tapering the waveguide causes the electric field to increase and assists in breakdown. The launcher in this case is basically the gap between the waveguide walls. Also, for MW discharges it is possible to use an electrode/antenna to produce the plasma. Some of the MW jets are based on this principle as shown in Figure 2.12d.

Typical wave-heated plasmas at atmospheric pressure operate at an elevated gas temperature (above 500 K) and have electron temperatures around 1–2 eV and electron densities in the range of 10^{20}–10^{21} m^{-3} (van der Mullen et al. 2007), although the electron density can be larger as it depends strongly on the power input.

2.9 Corona Discharges

Corona discharges are localized discharges in the neighborhood of a pin or a thin wire, where the field is significantly enhanced. Ionization and emission thus occurs locally around the pin or the wire. Corona discharges normally do not extend up to the counter electrode. For this reason a corona discharge is also known as a partial discharge. Two typical configurations of a corona discharge are shown in Figure 2.13a and b. A corona driven by a positive (negative) pin/wire electrode is called a positive (negative) corona. In the case of DC coronas the electrode gap can be divided into two zones: the high electric field region in which high-energetic electrons are produced and the ion drift region in which the electric field is low and the continuity of current toward the second electrode is guaranteed by a flux of positive ions (in the case of positive corona) or negative ions produced by electron attachment to, for example, oxygen (in the case of a negative corona). The morphology of the discharge is highly dependent on polarity and the applied voltage. This can also be seen in the current waveforms, which show that several of these corona discharges are highly dynamic in nature.

Negative DC corona can exhibit pulses. These pulses are called Trichel pulses and are caused by the space charge buildup produced by the corona. As the removal of the space charge (negative ions) is necessary to allow the next pulse, the frequency of the current pulses is typically of the order of 1–100 kHz. At a certain time-averaged current amplitude (or voltage) the negative corona becomes a continuous glow corona and the pulsation of the discharge stops. The current can be increased during this regime until a glow discharge is formed. This glow discharge is normally unstable and constricts to a spark. The stability region of the negative corona is thus determined by the threshold of the glow-to-spark transition.

Positive coronas can operate in a glow-like regime but are often intermittent and pulsed. For the larger current range the positive corona is streamer-like and the stability region is limited by the streamer-to-spark transition, which occurs when a streamer reaches the second (grounded) electrode.

In spite of the fact that the morphology of the negative and positive corona can be rather different, the time-averaged *I–V* characteristic is very much the same and is determined by the drift zone.

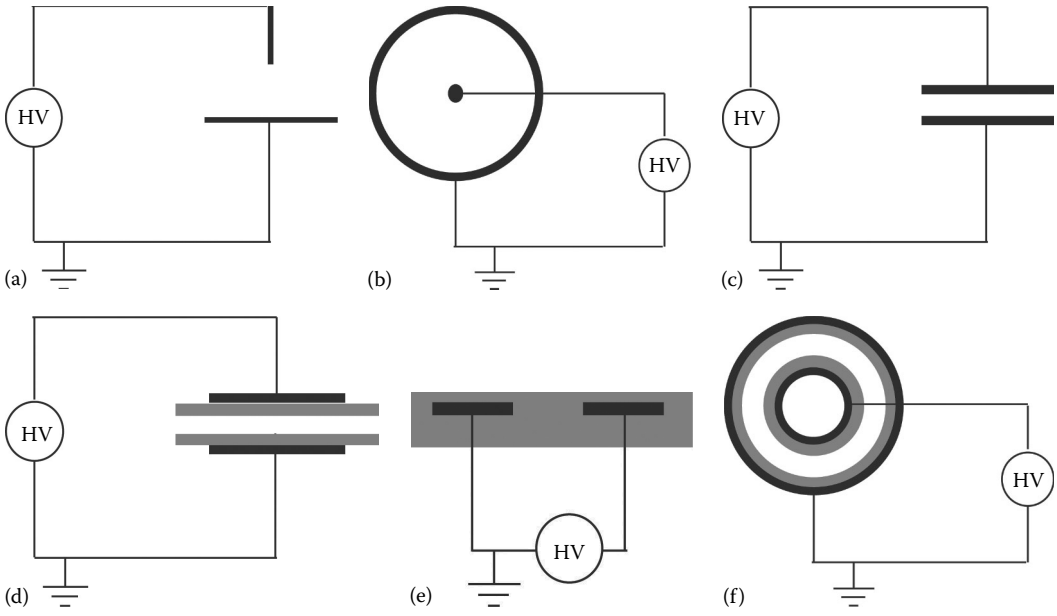

FIGURE 2.13 Different configurations to produce non-LTE plasmas at atmospheric pressure: (a) pin–plate corona geometry, (b) coaxial wire–cylinder corona geometry, (c) parallel-plate capacitively coupled RF discharge geometry, (d) parallel-plate DBD geometry, (e) surface DBD geometry, and (f) coaxial DBD geometry as used in ozone production applications.

The I–V characteristic can be analytically determined by solving the Poisson equation and the continuity of the current in the drift region in a wire–cylinder geometry assuming that space charge effects are small. Even in a general geometry the following I–V relation holds (Raizer 1987):

$$I = \mathrm{K}V(V - V_c),$$

where

K is a constant depending on the geometry and the mobility of the charge carriers in the drift zone
V_c is the threshold voltage for corona onset

The ignition voltage of the DC corona discharge depends on the polarity. This is easy to understand as in the case of the negative polarity the criterion for Townsend breakdown can be applied, while this is not the case for a positive corona as secondary electron emission does not occur at the pin/wire electrode. In this case the Meek criterion is considered for corona onset.

DC coronas are extensively used in electrostatic precipitators. Basically the ions in the drift region charge the dust particles, which are attracted by the grounded electrode and as such transported to the grounded electrode and removed from the exhaust gases.

Corona discharges are also used for air treatment such as removal of NO_x or volatile organic compounds (VOCs) (Chang et al. 1991). The energetic electrons in the corona produce radicals that can convert unwanted products in the gas stream into less harmful products or products that are easier to remove from the gas phase. For air treatment nanosecond pulsed discharges are mostly used. Nanosecond pulsing has several advantages that are correlated to the fact that the corona can be operated at much higher voltages compared to the DC case without spark formation, given that the voltage is switched off before the streamer-to-spark transition can occur. Higher voltages also leads to longer streamers that have a better filling ratio of the electrode gap and enables a more homogeneous treatment. Larger voltages lead to higher electric fields and electron temperatures, which increases ionization and dissociation rates. Additionally, due to the short pulse only electrons are significantly accelerated in a few nanoseconds, and gas heating can be kept to an absolute minimum.

Pulsed coronas or streamers have been investigated in detail and the basic mechanisms are now understood. In the case of negative streamers electron avalanches can cause the propagation of the streamer as the streamer develops in the same direction as the avalanches. Also, electron avalanches cause the propagation of positive streamers but it is generally accepted that photoionization in gas mixtures such as air plays an important role in generating electrons in front of the streamer head. Most streamers are highly branched. Inhomogeneities can explain branching (Babaeva and Kushner 2009), while a Laplacian instability of

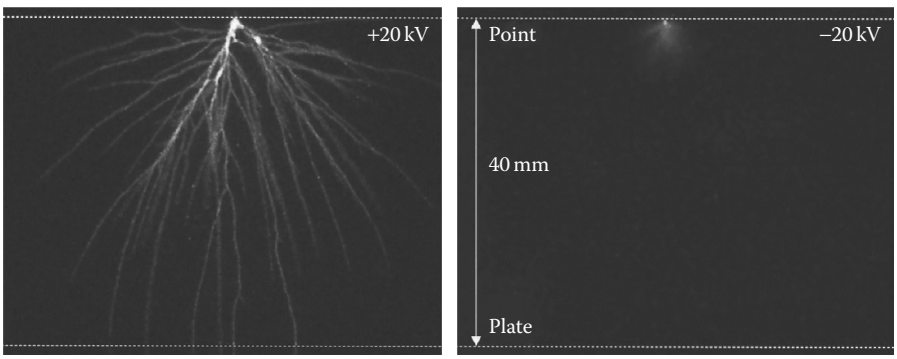

FIGURE 2.14 Example of a positive and negative corona discharge in a point–plate geometry with a gap of 40 mm. The needle is at the top of the image and a clear difference is seen for positive and negative streamers. (Reprinted with permission from Briels, T.M.P., et al., *J. Phys. D Appl. Phys*., 41, 23400, 2008, © IOP.)

the streamer head can theoretically explain branching (Arrayas et al. 2002) without the necessity of a inhomogeneity, which almost always occurs. As shown in Figure 2.14 a positive and a negative corona have a significantly different morphology even when excited by the same voltage pulse. The electron temperature is very large during the streamer propagation time up to the ionization energy of the gas and more and the typical electron density in streamers is often 10^{20}–10^{21} m^{-3} (Spyrou et al. 1992; Liu et al. 2007). Note that the chemistry in transient streamer discharges is a two-step process. During streamer propagation, excitation, ionization and dissociation occur, and excited species, metastables, radicals, electrons, and ions are produced. These highly reactive or energetic species subsequently recombine and react with molecules on a much longer timescale as the lifetime of a streamer. At this timescale also the main chemistry that is important for the applications happens.

2.10 RF Glow Discharges and Pulsed Diffuse Discharges

As discussed above, increasing the preionization in the gas leads to a larger avalanche density and interaction avalanches, because of which the conditions of the Meek criterion are not met. In relative high-frequency discharges or nanosecond pulsed discharges with a repetition frequency of more than 1 kHz this phenomenon can be important as the time between two subsequent discharges does not allow a full relaxation or recombination of the charge.

Diffuse glow discharge in atmospheric pressure helium with small admixtures (typically <2%) of molecular gases can be obtained in a capacitively coupled parallel-plate geometry even when bare metal electrodes are used (Figure 2.13c). Operating the discharge in the same reactor in other gases normally leads to a contraction of the discharge to a single filament with a significant increase in gas temperature. The electron density of the discharge is of the order of 10^{16}–10^{17} m^{-3} (Waskoenig et al. 2010), for which diffusive losses are still important. The discharge operates in the so-called alpha mode, which means that the main electron production/heating is in the gas phase (sheath region) rather than due to secondary electron production (gamma mode). The electron temperature in these discharges is typically in the range of 2–3 eV. This discharge configuration is very much appreciated by modelers as it can be well described by a one-dimensional code. Indeed, it is diffuse and behaves very much like a low-pressure glow discharge.

Nanosecond pulsed glow discharge are often produced at kilohertz frequencies in pin–pin geometries. Intrinsically, they can be produced at lower voltages compared to "single shot" glow discharges due to the significant memory effect, but they can still operate at voltages that would lead long pulses to a glow-to-spark transition, as shown in Figure 2.4. This is because these glow discharges have a higher power density compared to their DC counterparts and also often a larger electron density (typically 10^{19} m^{-3} or larger) (Pai et al. 2009). They are often investigated in the context of plasma-assisted combustion. However, there is a trend in the plasma-enhanced combustion field to move toward shorter and shorter voltage pulses, which does not allow time for the formation of a sheath, and only an ionization front travels across the electrode gap.

2.11 Dielectric Barrier Discharges

As already mentioned, the introduction of dielectric barriers between the metal electrode and the plasma can be used to reduce the current. The displacement current through the dielectric causes the continuity of the current in the circuit so in this case the discharge has to be driven by AC or pulsed voltage excitation. In the case of a DBD in general at least one of the metal electrodes is covered by a dielectric barrier and often both electrodes are. DBDs have been generated in parallel-plate or in coaxial cylindrical reactor geometries (Figure 2.13 d and f). Surface DBDs propagating over a dielectric surface are produced when, for example, both metal electrodes are encapsulated in the same dielectric material as shown in Figure 2.13e.

DBDs can operate in a diffuse mode or a filamentary mode (Figure 2.15). The most common morphology is a filamentary mode as in air or O_2. In this case a small filament, very much like a streamer, is locally produced and bridges the gap. Typically, because of the dielectric nature of the electrode,

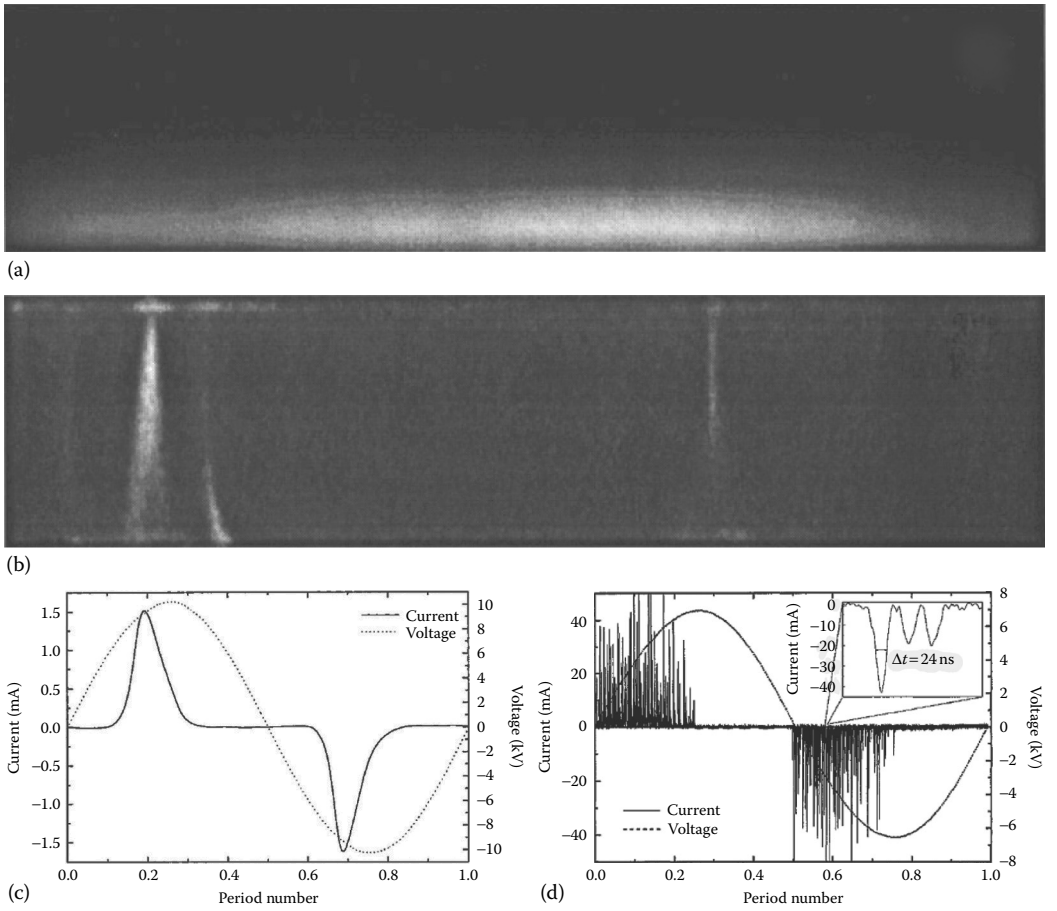

FIGURE 2.15 (a) and (b) Diffuse and filamentary DBD in N_2 with a gap of 4 mm and a voltage of 11 and 14 kV, respectively. (c) and (d) Typical current and voltage waveform of a diffuse and filamentary DBD. In the case of the filamentary discharges the current peaks produced by the microdischarges are clearly visible. (Reprinted with permission from Gherardi, N., et al., *Plasma Sources Sci. Technol.*, 9, 340–346, 2000, © IOP.)

the filament propagates partly over the electrode surface and often has a large contact area with the dielectric. In this process the filament transfers charge from one dielectric to the other and reduces the field locally. This leads to a memory effect, which causes the next filament to be produced at a different location. This phenomenon causes a spreading of the filaments, making the DBDs look diffuse with the naked eye even when they consist of many filaments.

These filaments behave as microchemical reactors. One of the most successful and oldest applications of DBDs is in ozone formation. Werner von Siemons reported the first experimental investigations more than 150 years ago (Siemens 1857). Ozone formation requires that three criteria be met: energetic electrons that are able to efficiently dissociate O_2 (4–5 eV), high pressure because of the three-body reaction, which is responsible for the ozone production, and low gas temperatures because of the reduced lifetime of O_3 at elevated gas temperatures. DBDs can deliver all these requirements as the gas temperature of the bulk gas can be maintained close to room temperature (for larger powers cooling of the electrodes is required), while the electron temperature is typically 2–5 eV. The electron density is reported to range from 10^{17} m^{-3} in the diffuse mode up to 10^{21} m^{-3} in the filamentary mode (Dong et al. 2008; Zhu et al. 2009).

The stabilization by the dielectric barriers makes the discharge very robust to instabilities, which lead to constriction, heating, and large current sparks/arcs even in electronegative gases such as oxygen.

An additional advantage is that the stabilizing component (the dielectric) is a capacitor that in the ideal case does not consume energy. This is a major advantage compared to discharges that are stabilized by resistors. Moreover, DBDs can easily be scaled up from small laboratory reactors to large industrial installations.

As stated above, most DBDs consist of filaments. However, there exist diffuse DBDs for specific conditions (see Figure 2.15b). The current waveform gives a good indication if one deals with a filamentary or diffuse discharge (Figure 2.15c and d). Diffuse discharges are easily obtained at reduced pressures or in He-rich mixtures. Plasma chemistry has a major effect on filamentation. As discussed above, a reduction in the ionization coefficient leads to diffuse discharges. Note that the high energy of He metastables causes most impurities to be ionized by Penning ionization. Many of the plasma jets used in biomedical applications are DBDs that are converted into a jet by applying a gas flow.

2.12 Microplasmas

Microplasmas are plasmas with dimensions of a few micrometers up to a few millimeters. As the typical cathode sheath thickness of a glow discharge at 1 mbar is of the order of 1 cm and at atmospheric pressure of the order of 100 μm, it is clear that microplasmas mostly operate under atmospheric pressure conditions. Unlike large-scale discharges at atmospheric pressure, microplasmas are strongly influenced by boundary-dominated phenomena. This behavior is very similar to that of low-pressure discharges given that microplasmas operate at similar pressure–distance (pd) values.

The effect that "microcavities" have on a plasma can be illustrated by the well-known microhollow cathode discharge. The microhollow cathode discharge is basically a DC-excited discharge in which the cathode is a metal tube (inner diameter D) and the anode a normal plate. When it operates at small currents, the discharge has the cathode sheath outside the tube, such as when using two parallel-plate electrodes. However, for increasing currents in the pressure range $pD \sim 0.1$–10 Torr cm, the cathode sheath enters the inner tube and a cathode sheath is formed along the inner tube wall. This causes the electrons to move back and forth between the sheaths at the inner walls (pendulum effect). The electrons are trapped significantly longer and cause more ionization before exiting the tube and moving toward the anode. As a result the plasma density increases for this type of cathode.

The main reason behind using microscale geometries at atmospheric pressure is that high-pressure plasmas, which typically have a tendency to constrict or undergo filamentation and excessive heating, are stabilized. The surface-to-volume ratio is increased in microgeometries and thermal gradients also increase, which leads to an increased heat transfer to the walls and electrodes. This consequently reduces the risk of thermal instabilities significantly. Additionally, as the size of the discharge is of the same order of magnitude as the cathode sheath (~100 μm), glow discharges can be operated without a (fully developed) positive column. As a positive column has the tendency to contract at large currents, the discharges can often be operated at higher densities without the risk of instabilities.

Amazingly, microplasma arrays are used to create large-volume diffuse APPs (Kunhardt 2000). With a microplasma in a three-electrode geometry, it is possible to generate a glow discharge with dimensions of a few cubic centimeters even in atmospheric pressure air (Mohamed et al. 2002). Figure 2.16 shows the conceptual geometry. A microplasma is used as a virtual cathode and the electrons are extracted from the microplasma by the anode, creating a diffuse low-density glow discharge.

Many different configurations of microplasmas exist but they are a scaled-down version of one of the types of discharges treated in the previous sections. Plasma densities can span a large parameter range as both plasma jets used for biomedical applications, which are often DBD-like plasma, and continuous micro DC-excited glow-like discharges are considered. The latter discharges operate with electron densities of the order of 10^{21} m^{-3} and with temperatures reaching 1000 K (Belostotskiy et al. 2010). One of the most popular applications of microplasmas are plasma display panels and UV (excimer) sources (Kogelschatz 2003).

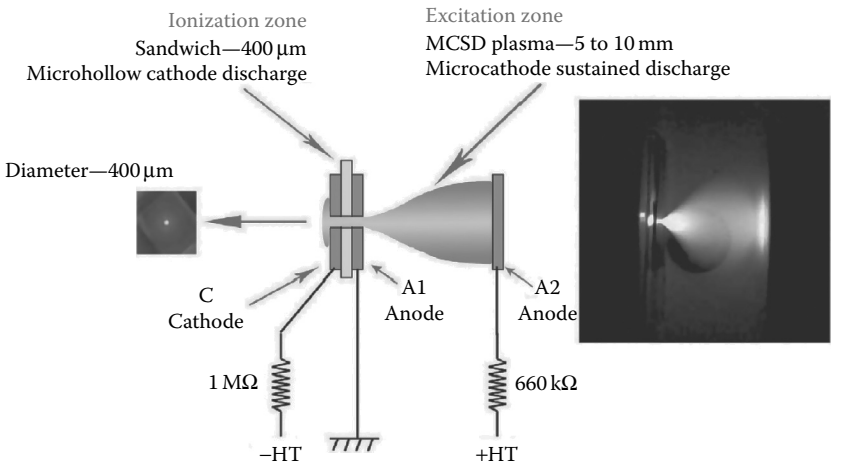

FIGURE 2.16 Microdischarge in three-electrode arrangement to produce large-volume diffuse atmospheric pressure discharges. (With kind permission from Springer Science+Business Media: *Eur. Phys. J. Appl. Phys.*, Microplasmas: Physics and application to the production of singlet oxygen $O_2(a^1\Delta_g)$, 42, 2008, 17–23, Puech, V.)

2.13 Conclusion

A wide variety of different APPs exist, which range from Townsend discharges up to thermal arcs, which span a range of ionization degrees of almost 10 orders of magnitude. The mean electron energies can be equal to the ionization energy of the gas in streamers up to close to room temperature in recombining room temperature plasmas. The gas temperatures typically range from ambient room temperature up to more than 1 eV. Because of the wide range of plasma properties, APPs have widespread applications ranging from cutting steel plates by a thermal arc to using cold APPs for wound treatment. At atmospheric pressure significant heating is most common although LTE conditions are an exception rather than the rule. To prevent heating, time-modulated plasmas have to be used. The large variety of plasma properties, chemistry, and applications make APPs a very fertile topic for both fundamental and application-oriented studies. Additional complexity is even obtained when a liquid phase is added (Bruggeman and Leys 2009b). The complex plasma chemistry that normally exists at application conditions in combination with the self-organizing nature and filamentation of APPs provides us with many interesting and challenging unresolved scientific questions.

References

Arrayas, M., Ebert, U., and Hundsdorfer, W. 2002. Spontaneous branching of anode-directed streamers between planar electrodes. *Phys. Rev. Lett.* 88 (17): 174502.

Babaeva, N.Y. and Kushner, M.J. 2009. Effect of inhomogeneities on streamer propagation: I. Intersection with isolated bubbles and particles. *Plasma Sources Sci. Technol.* 18 (3): 035009.

Barinov, Y.A., Kaplan, V.B., Rozhdestvenskii, V.V., and Shkol'nik, S.M. 1998. Determination of the electron density in a discharge with nonmetallic liquid electrodes in atmospheric pressure air from the absorption of microwave probe radiation. *Tech. Phys. Lett.* 24 (12): 929–931.

Belostotskiy, S.G., Ouk, T., Donnelly, V.M., et al. 2010. Gas temperature and electron density profiles in an argon DC microdischarge measured by optical emission spectroscopy. *J. Appl. Phys.* 107: 053305.

Boulos, M.I., Fauchais, P., and Pfender, E. 1994. *Thermal Plasmas: Fundamentals and Applications*. New York: Plenum.